Bioorg. Med. Chem. 31 (2021) 115976

Contents lists available at ScienceDirect

Bioorganic & Medicinal Chemistry

journal homepage: www.elsevier.com/locate/bmc

Synthesis, anticancer and antimicrobial evaluation of new benzofuran based derivatives: PI3K inhibition, quorum sensing and molecular modeling study

Omar A. El-Khouly [a], Morkos A. Henen [a,b,*], Magda A.-A. El-Sayed [a,c], Mona I. Shabaan [d], Shahenda M. El-Messery [a,*]

[a] Department of Pharmaceutical Organic Chemistry, Faculty of Pharmacy, Mansoura University, P.O. Box 35516, Mansoura, Egypt
[b] Department of Biochemistry & Molecular Genetics, University of Colorado, Denver, USA
[c] Department of Pharmaceutical Medicinal Chemistry, Faculty of Pharmacy, Horus University, P.O. Box 34518, New Damietta, Egypt
[d] Department of Microbiology and Immunology, Faculty of Pharmacy, Mansoura University, P.O. Box 35516, Mansoura, Egypt

ARTICLE INFO

Keywords:
Benzofuran
Hybridization
Anticancer
Antimicrobial
PI3K
Quorum sensing
Molecular modeling
NOESY

ABSTRACT

A new series of benzofuran derivatives has been designed and synthesized. The structures of the synthesized compounds have been confirmed by the use of ^{1}H NMR, ^{13}C NMR, 2D ^{1}H–^{1}H NOESY NMR, and IR. Anticancer activity is evaluated against Hepatocellular carcinoma (HePG2), mammary gland breast cancer (MCF-7), Epitheliod carcinoma cervix cancer (Hela) and human prostate cancer (PC3). Compounds **8**, **9**, and **11** showed the highest activity towards the four cell lines with an IC_{50} range of 8.49–16.72 μM, 6.55–13.14 μM and 4–8.99 μM respectively in comparison to DOX (4.17–8.87 μM). Phosphatidylinositol-3-kinases (PI3K) inhibition was evaluated against the most active anticancer compounds **8**, **9** and **11**. Compounds **8**, **9** and **11** showed good inhibitory activity against PI3Kα with IC_{50} values 4.1, 7.8, and 20.5 μM, respectively in comparison to 6.18 μM for the reference compound LY294002. In addition, activity of compounds **8** and **9** on cell cycle arrest and induction of apoptosis in different phases of MCF-7 cells were assessed and detected pre-G1 apoptosis and cell growth arrest at G2/M. Also, both extrinsic and intrinsic apoptosis in MCF-7 cells induced by compounds **8** and **9.** Molecular docking, binding affinity surface mapping, and contact preference of the synthesized compounds **8**, **9** and **11** against PI3K were estimated and studied computationally using molecular operating environment software (MOE) and showed good interaction with essential residues for inhibition Val851. In addition, antimicrobial activity was evaluated against gram positive isolates as *Staphylococcus aureus* and *Bacillus cereus,* gram negative isolate as *Escherichia coli*, *Pseudomonas aeruginosa* and antifungal potential against *Candida albicans*. Compound **17** showed outstanding anti Gram-positive activity with MIC values 8 and 256 μg/mL in *Staphylococcus aureus* and *Bacillus cereus* respectively. Also, compounds **15**, **17**, **18** and **21** showed good anti Gram-negative activity with MIC value 512 μg/mL for all compounds. In addition, the state-of-art quorum sensing (QS) inhibiting effects were detected using *Chromobacterium violaceum* and compounds **7**, **9**, **10**, **11**, and **12** showed good QS inhibition (3, 3, 5, 2, and 7 mm).

1. Introduction

In 2020, the American Cancer Society expects that approximately 2 million new cases of cancer with 600 thousand deaths in the United States of America (USA) only.[1] To date, cancer management protocols are either via resection, transplantation or using the chemotherapeutic agents that have severe impact on the human healthy cells.[2] The hazard on normal cells and resistance to the current chemotherapy protocols create the urgent need to research, design and synthesis of novel anticancer agents which have better activity and tolerability.[3] Phosphatidylinositol-3-kinases (PI3K) pathways play an important role for regulation of cell proliferation, growth, survival, differentiation, motility, angiogenesis and apoptosis[4,5] and significantly overexpressed in cancer and some respiratory inflammations.[6] Alpelisib, a thiazole containing drug, is the first PI3K inhibitor which was approved by FDA for treatment of breast cancer in May 2019.[7] Aberrant activation of PI3K

* Corresponding authors at: Department of Pharmaceutical Organic Chemistry, Faculty of Pharmacy, Mansoura University, P.O. Box 35516, Mansoura, Egypt.
E-mail addresses: morkos.henen@ucdenver.edu (M.A. Henen), selmessery@gmail.com (S.M. El-Messery).

https://doi.org/10.1016/j.bmc.2020.115976
Received 19 September 2020; Received in revised form 16 December 2020; Accepted 21 December 2020
Available online 27 December 2020

has been widely implicated in many cancers and increased the activity of this pathway is often implicated in resistance to cancer therapy. In cancer cells, uncontrolled signaling through PI3K can occur by multiple mechanisms such as mutation, amplification of tyrosine kinase or PI3K itself.[8,9] PI3K signaling is initiated by the growth factor that binds to the tyrosine kinase receptor leading to receptor dimerization. As a consequence, lipid kinase PI3K is recruited to the internal docking site and become activated. Then, PI3K converts membrane lipid phosphatidylinositol 4,5-bisphosphate 2 (pip2) to its active Phosphatidylinositol 4,5-bisphosphate 3 (pip3) which in turn leads to activation of key signaling kinase Protein kinase B (AKT).[10] AKT promotes cell growth through protein synthesis driven by mammalian target of rapamycin (mTOR) signaling and reduce cell death by blocking Forkhead box o class protein (FOXO) activity which enhances translation and inhibits the apoptosis.[9,11] In 2018, World Health Organization (WHO) announced that the antibiotics resistance is one of the biggest threats to human life.[12] Antibiotics resistance is the cause of over than 33,000 deaths in European Union in 2015.[13] So, we need to discover new antimicrobial compounds to fight resistant organisms. Benzofuran derivatives showed a proven antimicrobial activity.[14–17] In this study, antimicrobial activity was evaluated for the newly synthesized compounds.

Quorum Sensing (QS) is a technique used by microbes to perform cell–cell communications through autoinducers which is a chemical signal released by microbe.[18] Bacteria produce signal molecules called autoinducers that they capable of communicating and controlling processes like biofilm formation and antibiotic resistance.[19] The use of molecules to confuse bacterial contact and virulence may therefore lead to frustrating bacterial tolerance and to provide that successful conventional treatment.[20] Considering drug discovery approaches, hybridization is an effective strategy in drug design. It's applied to make a fusion between two pharmacophore moieties in previously reported active compounds.[21] Benzofuran containing compounds as ebenfuran I, II, and III which are natural compounds showing significant activity against some types of cancer.[22] As well as thiazole derivatives have significant anticancer activity as FDA approved, Alpelisib, and synthetic thiazole derivative, TAP-07, which synthesized and shows a significant *in vivo* and *in vitro* activity against breast cancer.[23] In addition, piperazine (compound A) and hydrazone (compound B) derivatives have anticancer activity.[24,25] Also, hydrazo and azo groups have been reported as antimicrobial activity enhancer[26–29] (Fig. 1).

In this study, we aimed to design and synthesis a novel benzofuran-thiazole, benzofuran-azo, benzofuran-hydrazo, and benzofuran-piperazine hybrids and assess their activity as anticancer and antimicrobial drugs (chart 1). The synthesized compounds were assessed for *in vitro* cytotoxicity against a panel of four tumor cell lines, namely, hepatocellular carcinoma (HePG2), mammary gland breast cancer (MCF-7), epithelioid carcinoma cervix cancer (Hela) and human prostate cancer (PC3). Although, the safety index was assessed *in vitro* using human lung fibroblast (WI38) cell line. Furthermore, the most potent compounds were tested for their effect on cell cycle distribution and apoptosis in addition to the enzymatic inhibitory potency on PI3K as a promising mechanism of their anticancer activity. In addition, the newly synthesized compounds were assessed for antimicrobial activity and determine minimal inhibitory concentrations for the active compounds against Gram positive organisms such as *Bacillus cereus* UW85, *Staphylococcus aureus* ATCC 29,213 and against Gram negative isolates including *Escherichia coli* ATCC 12435, *Pseudomonas aeruginosa* PAO1. Furthermore, the antifungal potential of the compound was evaluated against *Candida albicans CS351*, and QS inhibitory concentration against *Chromobacterium violaceum*.

2. Result and discussion

2.1. Chemistry

2-(1-(Benzofuran-2-yl)ethylidene)hydrazinecarbothioamide **(3)** was utilized as a starting material in benzofuran-thiazole hybrids and it was synthesized as shown in Scheme 1. 2-Acetyl benzofuran **(2)** is synthesized by reaction of salicylaldehyde with chloroacetone in dry acetone in presence of potassium carbonate.[30] Carbonyl group of compound **2** was reacted with thiosemicabazide (TSC) in ethanol with catalytic amount of glacial acetic acid to give thiosemicarbazone **3**[31] (Scheme 1).

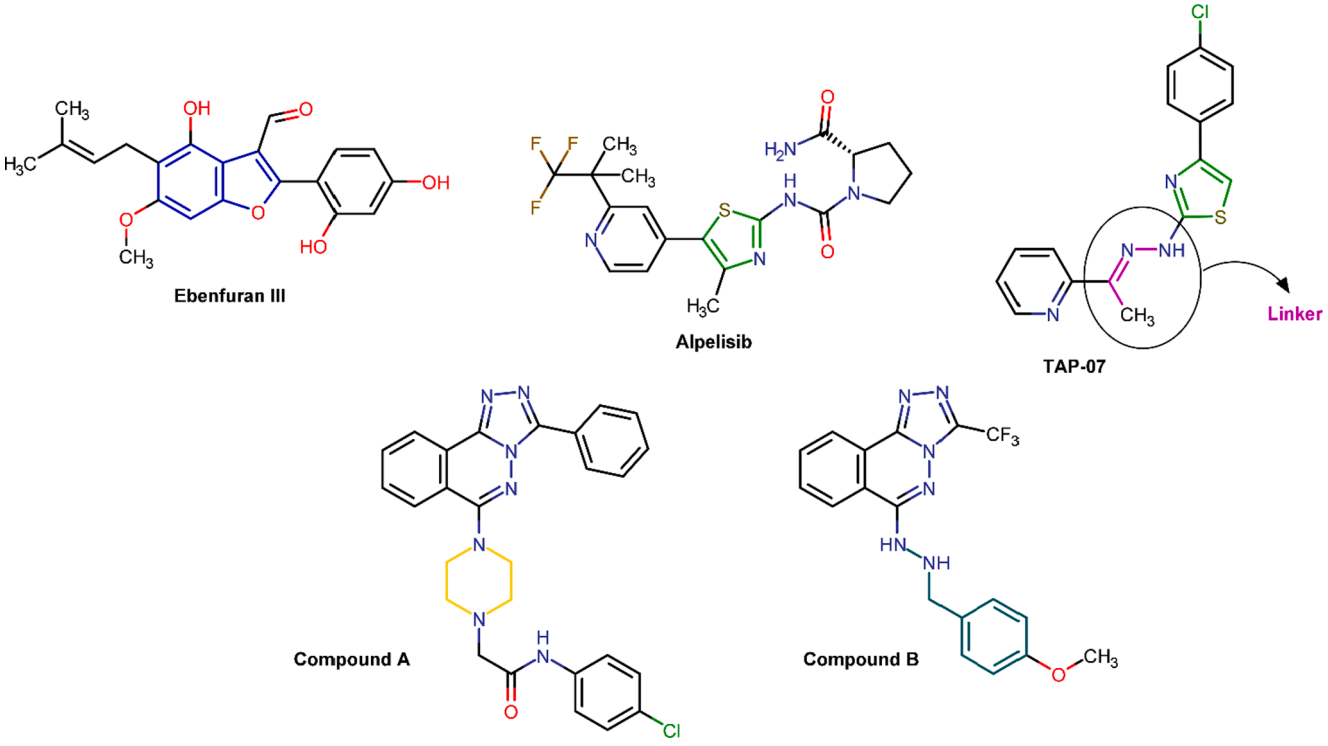

Fig. 1. Reported antitumor benzofuran, thiazole, piprazine, hydrazo compounds.

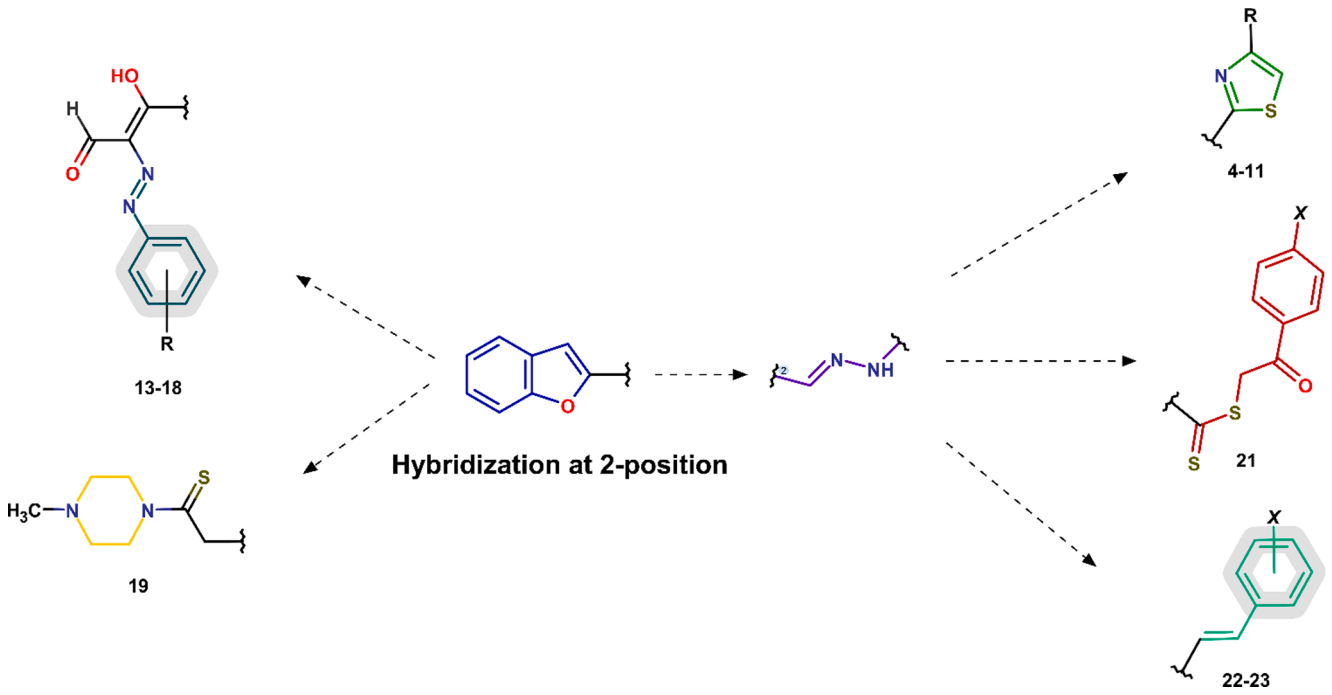

Chart 1. Design of novel benzofuran hybrids.

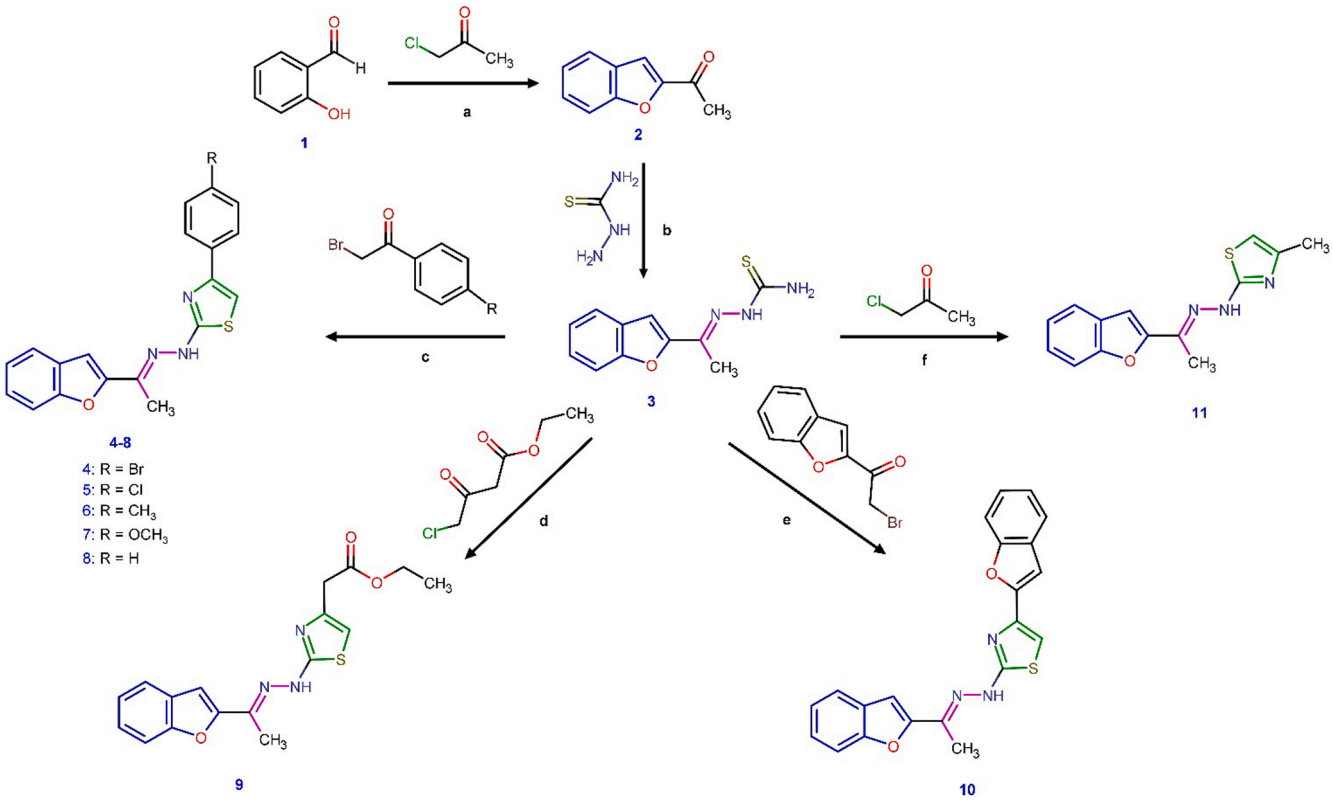

Scheme 1. Reaction conditions: (a) dry acetone, K_2CO_3, (b), (c), (d), (e) and (f) EtOH, glacial HOAc, reflux.

Thiosemicarbazone **3** is the key intermediate for the synthesis of thiazoles **4**–**11** *via* the reaction of α-haloketones as phenacyl bromide derivatives, 4-choloroacetoacetate, 2-bromoacetyl benzofuran and chloroacetone with thioamide in ethanol and catalytic amount of glacial acetic acid through Hantzsch thiazole synthesis according to reported procedure[32–35] to give 4-substituted thiazole with different moieties as *p*-substituted phenyl **4**–**8**, ethylethanoate **9**, benzofuran **10**, and methyl **11** derivatives respectively (Scheme 1).

The structure of the new compounds **4**–**11** were confirmed by ^{1}H NMR at δ: 7.10 to 7.47 (s, 1H) to singlet proton for all compounds of thiazole scaffold, δ: 7.91 to 7.24 (2CH) for compounds **4**–**8** phenyl moiety, δ: 2.33 (CH_3) for compound **6** of methyl protons of 4-

methylphenyl group, δ: 3.85 (CH_3) for compound **7** of methyl protons of 4-methoxyphenyl group, δ: 7.43 (CH) triplet peak for compound **8** of 4-proton of phenyl group, δ: 1.22 (CH_3) for compound **9** of side chain, δ: 7.10 (CH) for compound **10** benzofuran scaffold, δ: 1.56 (CH_3) for compound **11** of 4-methlythiazole group. Also, ^{13}C NMR spectral data of all compounds confirmed their structures. 2D ^{1}H–^{1}H homonuclear NOESY is important method to deep understanding of the relation between protons. It was recorded on 600 MHz NMR machine with 320 ms mixing time to confirm the structure of compound **7**. Strong cross peaks are observed between spins 7.8 and 7.02 & between 7.6 and 6.94 ppm (Fig. 2). Moreover, elemental analysis supported the expected structures.Fig 3.

The key intermediate 1-(benzofuran-2-yl)-3-(dimethylamino)prop-2-en-1-one **(12)** was utilized as a starting material in the second series of newly synthesized compounds and it was prepared by addition of dimethylformamide dimethylacetal (DMFDMA) to a solution of compound **2** in dry xylene.[36] Compounds **13**–**18** were synthesized by addition of aryldiazonium chloride to compound **12** in presence of sodium acetate to produce the desired hybrid as shown in Scheme 2.[37]

The structure of the new compounds **17**–**22** were confirmed by ^{1}H NMR at δ: 9.9 to 14.78 (exchangeable H) and new four aromatic proton for all compounds. Also, ^{13}C NMR spectral data of all compounds displayed ^{13}C peaks which confirms their structure. Moreover, elemental analysis supported the expected structures. It was found that diazotized aryl derivatives couples readily with the aminovinyl ketones to produce products of coupling and hydrolysis of dimethylamino moiety. The coupling products can thus be formulated as the hydrazone forms (*E*-form and *Z*-form) or potential tautomeric keto enol forms or a mixture of one or more of these forms as shown in Fig. 3.[38] Intramolecular hydrogen bond in compounds **13**–**18** is confirmed by ^{1}H NMR as shown in Fig. 4 which represented the chart of compound 13.

Willgerodt's reaction is used to synthesize novel benzofuran-piprazine hybrid by mixing of *N*-methyl piprazine to 2-acetyl benzofuran **(2)** in presence of sulfur and potassium carbonate in glycerol to produce compound **19** (Scheme 3).[39] (1-(Benzofuran-2-yl)ethylidene) hydrazine **(20)** is previously reported as intermediate for many reactions that contains primary amine which can intermediate many reactions.[40] Compound **20** was prepared by addition of hydrazine hydrate to 2-acetyl benzofuran **(2)** in ethanol.[40] Several procedures were reported for the synthesis of dithocarbamate derivatives. They can be prepared from the reaction of alkyl halide with carbon disulfide and secondary amine in presence of NaOH in DMF,[41] Cs_2CO_3 in acetone,[42] KOH in DMF,[43] or Na_3PO_4 in DMF.[44] In this study, compound **21** were synthesized by adding of carbon disulfide to compound **20** and alkyl halide in presence of anhydrous sodium phosphate in DMF to produce the desired hybrid **21** as shown in Scheme 3.[44]

Compounds 22 and 23 were prepared *via* Schiff-base condensation of adding primary amine (1-(benzofuran-2-yl)ethylidene)hydrazine **(20)** to a solution of appropriate aryl aldehyde derivative in absolute ethanol to produce desired derivatives **22** and **23** as shown in Scheme 3.[45]

The structure of the new compound 19 were confirmed by ^{1}H NMR at δ: 2.23 to 4.23 ($4CH_2$) of piprazine and δ: 2.25 (CH_3) of *N*-methyl group. The structure of the new compound 21 were confirmed by ^{1}H NMR at δ: 3.86 (CH_2) and the appearance of new four aromatic proton peaks. The structure of the new compounds 22–23 were confirmed by ^{1}H NMR at δ: 8.91 or 8.94 (s, CH) and new four aromatic proton for all compounds. Also, ^{13}C NMR spectral data of all compounds displayed ^{13}C peaks which confirmed their structure. Moreover, the IR spectra supported the expected structures of compounds **22** and **23** with the absence of two strong absorption band in region 3300–3500 cm^{-1} which was due to the primary amine in compound **20**. Compound **21** IR spectrum supported the expected structure with strong absorption band in region 1705–1725 cm^{-1} resulting from carbonyl group.

2.2. *In vitro antitumor evaluation using MTT assay*

All the newly synthesized compounds **4**–**11, 13**–**15** and **17**–**23** cytotoxicity were evaluated against four cancer cell lines using doxorubicin (DOX) as reference drug. The panel consisted of hepatocellular carcinoma (HePG2), mammary gland breast cancer (MCF-7), epitheliod earcinoma cervix cancer (Hela) and human prostate cancer (PC3). The cell lines were obtained from the American Type Culture Collection

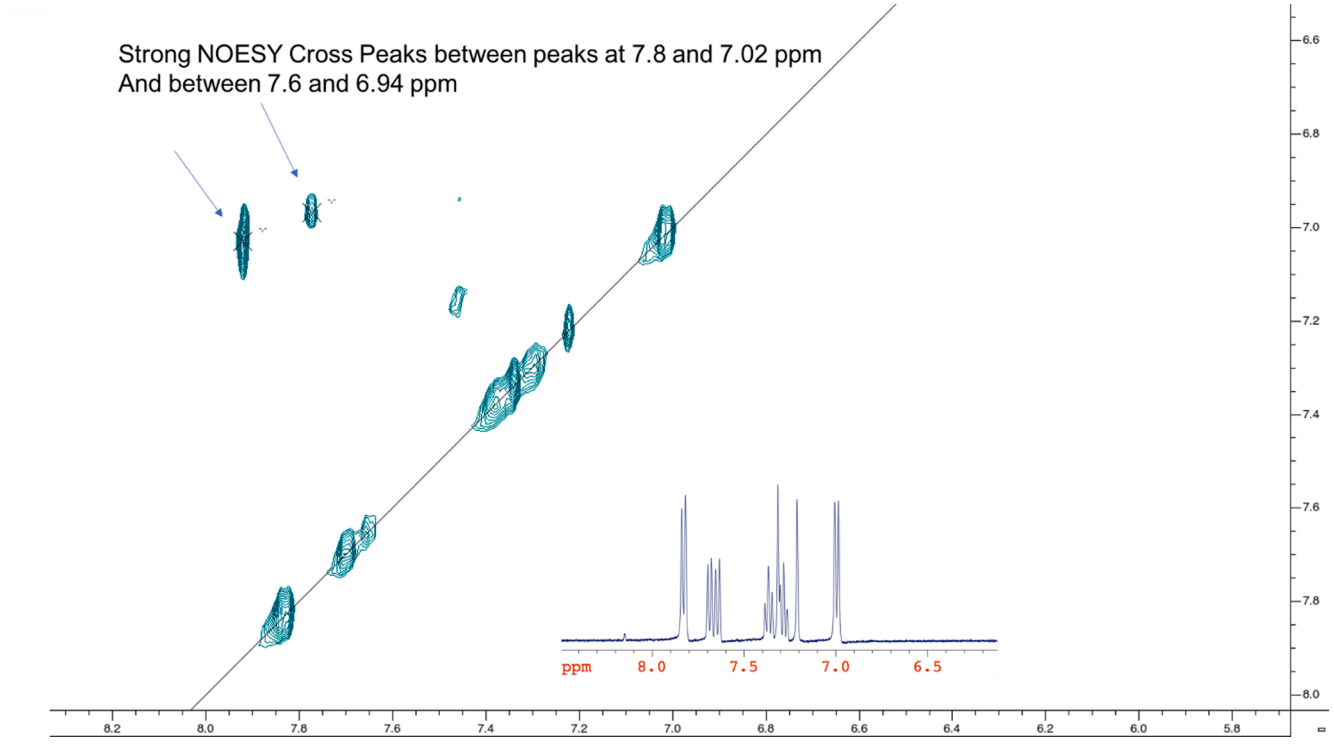

Fig. 2. 2D ^{1}H–^{1}H homonuclear NOESY of compound **7**.

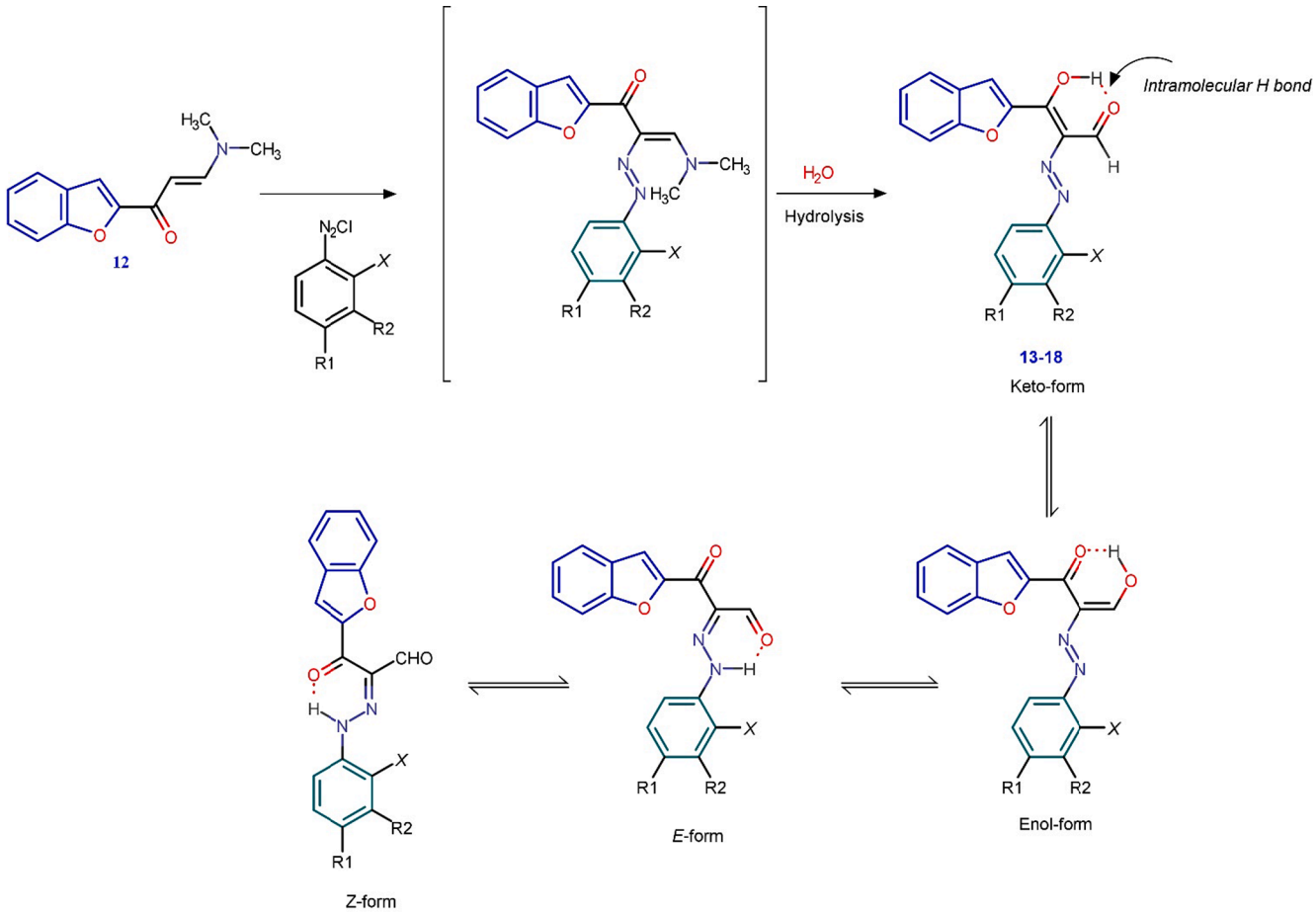

Fig 3. Equilibrium between compounds **13–18** forms.

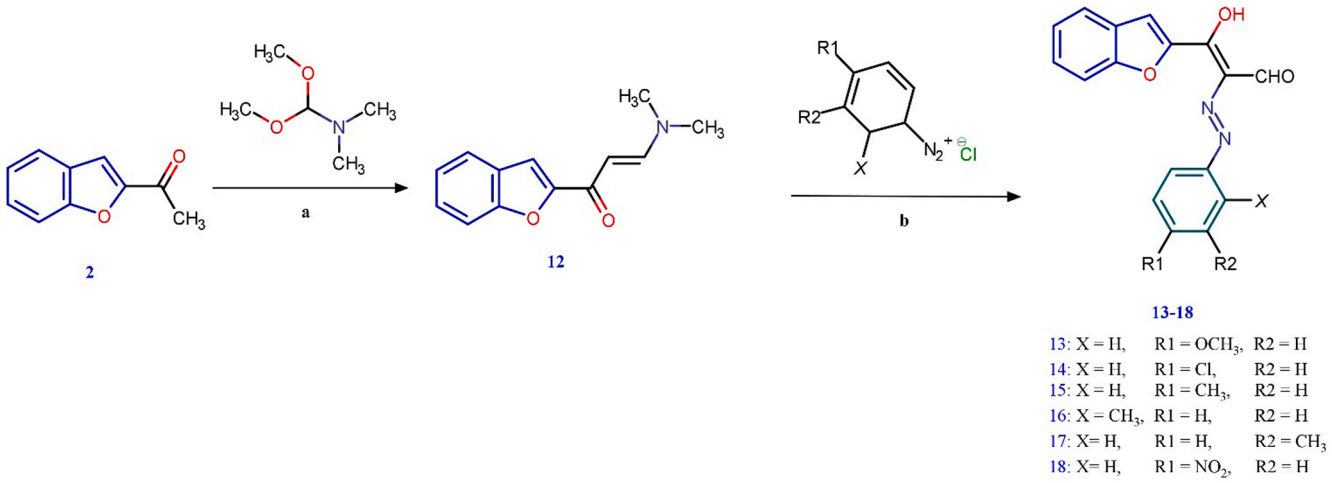

Scheme 2. Reaction conditions: (a) dry xylene, reflux, and (b) EtOH, NaOAc, r.t.

(ATCC) via Holding company for biological products and vaccines (VACSERA), Cairo, Egypt. The results are summarized in Table 1 and Fig. 5. The compounds which were synthesized by hybridization of benzofuran and thiazole pharmacophores **4**–**11** showed significant higher inhibition activity rather than other newly synthesized compounds. Compounds **8**, **9**, and **11** showed the highest activity with an $IC_{50\%}$ range of 8.49–16.72 μM, 6.55–13.14 μM and 4–8.99 μM respectively in comparison to DOX (4.17–8.87 μM). Compound **11** with 4-methyl substituted thiazole ring showed higher activity than all compounds that have 4-phenyl substituted thiazole ring. Substitution at position 4 with unsubstituted phenyl group is higher activity than substitution with open chin which is higher activity than *para*-substituted phenyl group and showed medium activity towards the four cell lines. Benzofuran-benzylidine, Benzofuran-dithiocarbamate, benzofuran-aryl hydrazone, and benzofuran-piperazine hybrids showed lower activity than benzofuran-thiazole hybrids. For benzofuran-thiazole hybrids, the activity towards the four cell lines can be arranged in ascending order as: *p*-Br, *p*-Cl, *p*-OCH_3, *p*-CH_3, then unsubstituted phenyl.

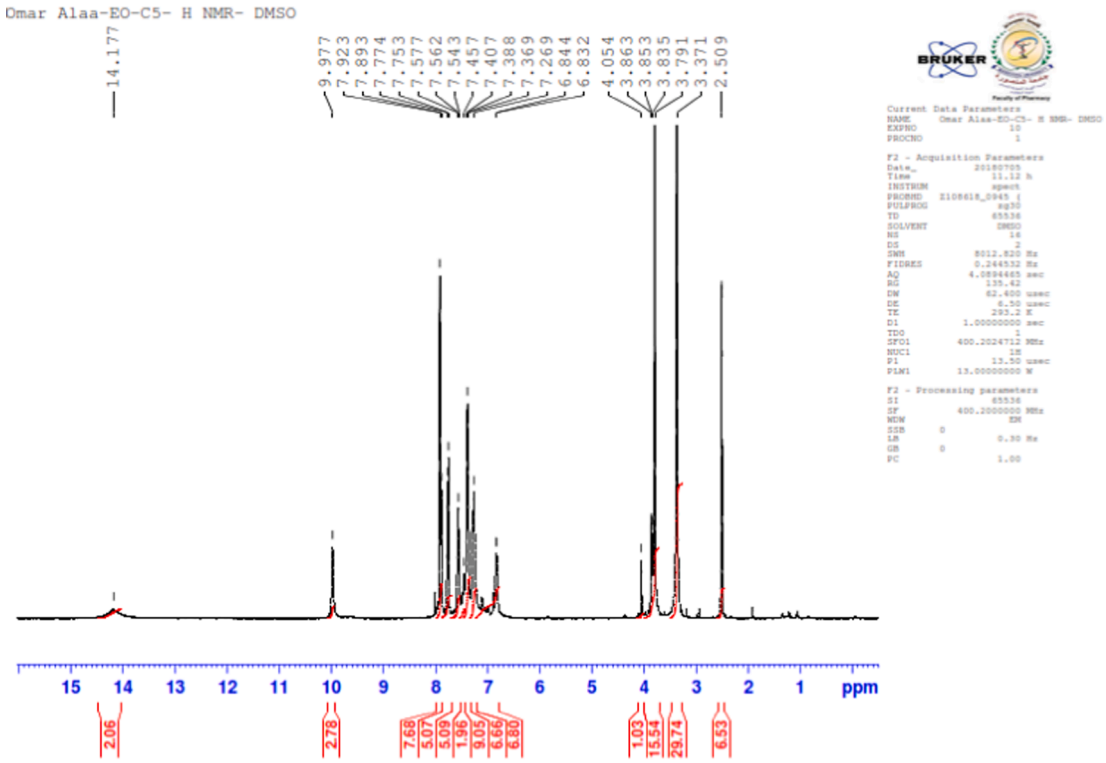

Fig 4. ^{1}H NMR of compound **13.**

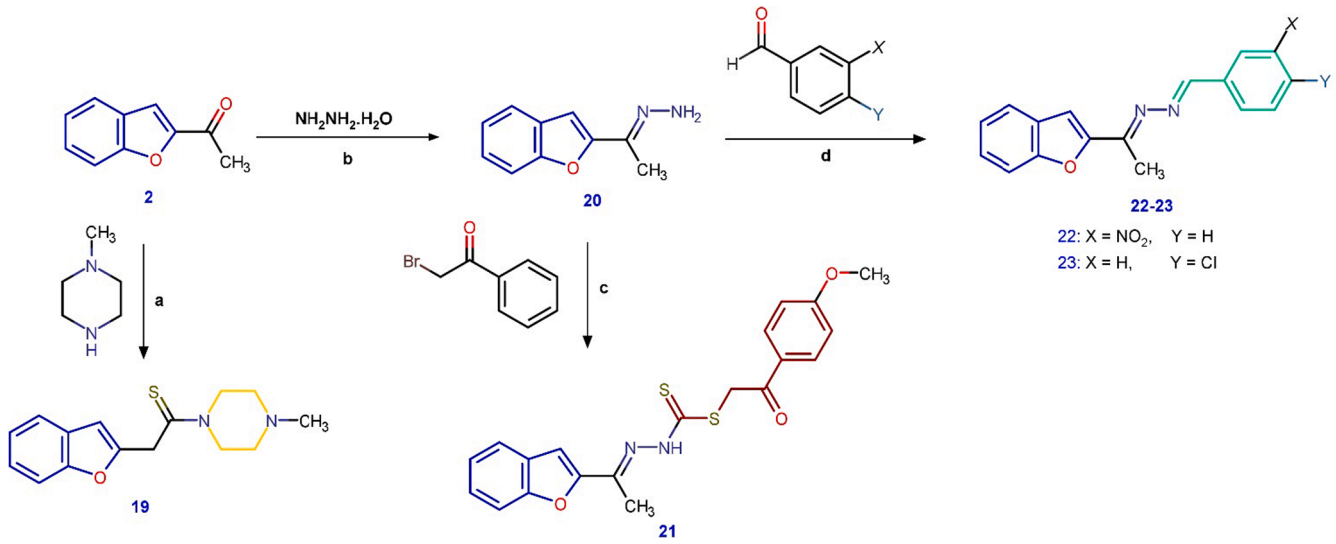

Scheme 3. Reaction conditions: (a) metallic sulfur, K_2CO_3/Glycerol (b) EtOH, 70 °C, (c) CS_2, Na_3PO_4, DMF, r.t. and (d) EtOH/HOAc, reflux.

2.3. *In vitro cytotoxicity against human normal cells*

Assessment of the selectivity of newly synthesized compounds between normal and cancer cell was performed. All compounds were evaluated against one of the available cell lines namely: Human lung fibroblast (WI38) cell line using doxorubicin (DOX) as a reference drug. The results are summarized in Fig. 6. The most active compounds **9**, **8** and **11** showed lower toxicity towards WI38 (IC_{50} = 36.77 μM, 41.70 μM and 44.31 μM, respectively) in comparison to DOX (IC_{50} = 6.72 μM) against WI38. Compound **13** (IC_{50} = 83.48 μM) had a lower toxic effect than DOX on the normal WI38 cells. Herein, the toxicity results on normal cell indicate that the most active compounds **9**, **8** and **11** have very strong activity toward the four tested cell lines with an $IC_{50\%}$ range of 4–8.99 μM, 6.55–13.14 μM and 8.49–16.72 μM respectively (DOX $IC_{50\%}$ range 4.50–8.87) but with higher safety index which is more than DOX ($IC_{50\%}$ = 6.72) by 5.5 to 6.6 folds on WI38 cell line with $IC_{50\%}$ 44.31, 41.70, and 36.77 respectively.

2.4. *Human PI3Kα enzyme inhibitory assay*

Compounds **8**, **9** and **11**, which display the highest activity against the four tested cancer cell lines, were assessed for their inhibitory activity against human PI3Kα enzyme relative to the reference compound LY294002, which is a potent PI3Kα inhibitory drug.[46] Compounds **8**, **9** and **11** showed good inhibitory activity against PI3Kα with IC_{50} values 4.1, 7.8, and 20.5 μM, respectively in comparison to 6.18 μM for

Table 1
In vitro antitumor activity (IC_{50}, μM) of the tested compounds and doxorubicin.

Compound	*In vitro* cytotoxicity IC_{50} (μM)			
	HePG2[a]	**MCF-7**[b]	**Hela**[c]	**PC3**[d]
4	27.72 ± 2.3	33.16 ± 2.8	32.72 ± 2.5	45.24 ± 2.9
5	23.18 ± 2.0*	29.88 ± 2.5	26.63 ± 2.3	38.10 ± 2.8
6	14.06 ± 1.3*	11.06 ± 0.9*	14.30 ± 1.2*	21.36 ± 1.7*
7	15.69 ± 1.5*	18.92 ± 1.6*	18.72 ± 1.7*	28.87 ± 2.2
8	10.31 ± 0.9†	8.49 ± 0.7†	11.71 ± 1.0*	16.72 ± 1.3*
9	7.74 ± 0.4†	6.55 ± 0.5†	9.26 ± 0.8†	13.14 ± 1.0*
10	21.25 ± 1.8	25.56 ± 2.2	24.13 ± 2.1	34.20 ± 2.6
11	4.00 ± 0.2 †	4.89 ± 0.3 †	8.97 ± 0.6 †	8.99 ± 0.7 †
13	42.10 ± 2.9	54.39 ± 3.5	59.19 ± 3.4	56.26 ± 3.5
14	37.29 ± 2.7	49.32 ± 3.5	38.22 ± 2.9	51.82 ± 3.3
15	46.76 ± 2.9	58.61 ± 3.7	63.25 ± 3.8	61.98 ± 3.7
16	52.27 ± 3.1	66.15 ± 3.9	69.43 ± 4.0	63.30 ± 3.9
17	72.37 ± 3.5	83.61 ± 4.3	75.02 ± 4.2	77.58 ± 4.3
18	35.36 ± 2.6	43.20 ± 3.3	37.82 ± 2.7	49.64 ± 3.1
19	64.53 ± 3.2	73.50 ± 4.1	87.03 ± 4.7	83.82 ± 4.5
21	31.88 ± 2.4	38.42 ± 3.0	46.94 ± 3.1	73.29 ± 4.1
22	77.36 ± 3.9	88.46 ± 4.6	>100	>100
23	86.55 ± 4.3	>100	>100	91.82 ± 4.9
DOX	4.50 ± 0.2	4.17 ± 0.2	5.57 ± 0.4	8.87 ± 0.6

a Hepatocellular carcinoma (HePG2). b Mammary gland Breast cancer (MCF-7).
c Epitheliod Carcinoma Cervix cancer (Hela).
d Human prostate cancer (PC3). IC_{50}: compound concentration required to inhibit tumor cell proliferation by 50% (Mean ± SD, n = 3).
IC_{50} (μM). †1-10 (very strong), *11–25 (strong), 26–50 (moderate), 51–100 (weak), >100 (non-toxic). DOX: doxorubicin as a reference drug.

compound LY294002 (Table 2). Compound **8** has the highest activity (IC_{50} = 4.1 μM) and has higher inhibitory activity than LY294002. The cytotoxicity compounds **8, 9,** and **11** against the four tested cancer cells showed an excellent matching with the enzymatic inhibition of PI3Kα parallel with the calculating docking interaction energy values. These results strongly suggested that the PI3Kα inhibitory mechanism might be one of the main modes of action of the anticancer activity of the synthesized compounds especially compound **8** with potent activity against PI3Kα.

2.5. Cell cycle arrest analysis

The good results of cytotoxicity and enzyme inhibitory assays led to the examination of the effect of compounds **8** and **9** on cell cycle distribution and induction of apoptosis in different phases of MCF-7 cells. MCF-7 cells were treated with compounds **8** and **9** for 24 h, stained with propidium iodide (PI), and analyzed by flow cytometer (FCM), the results are shown in Table 3 and Fig. 7. Compounds **8** and **9** decreased cell proportions at S phase to 29.57% and 33.71% respectively in comparison to the control cells (36.26%). Also, the results of compounds **8** and **9** showed that cells were arrested in G2-M phase of the cell cycle at 24 h by 30.82% and 22.34% respectively in comparison to the control cells (9.85%). Compounds **8** and **9** induced block in G0-G1 phase by 39.61% and 43.95% respectively in comparison to the control cells (53.89%). The induced apoptosis was determined by assessing the percent of cells blocked in the pre-G1 phase: 29.93% and 17.66% respectively of cells were found in the pre-G1 phase after 48 h exposure of **8** and **9** respectively compared to the control cells (1.78%).

2.6. Detection of apoptosis

Both extrinsic and intrinsic apoptosis in MCF-7 cells induced by compounds **8** and **9** were also assessed by Annexin V and PI staining. In this study, MCF-7 cells were incubated with **8** and **9** for 24 h. Compounds **8** and **9** was found to induce an early apoptotic effect 5.92% and 3.27% in MCF-7 at 24 h respectively and to enhance late apoptotic induction 14.65 and 8.1% by 98-fold and 54-fold respectively compared to the control cells (0.15%). Cumulatively, compounds **8** and **9** induced apoptosis with 29.93% and 17.66% respectively, the results are shown

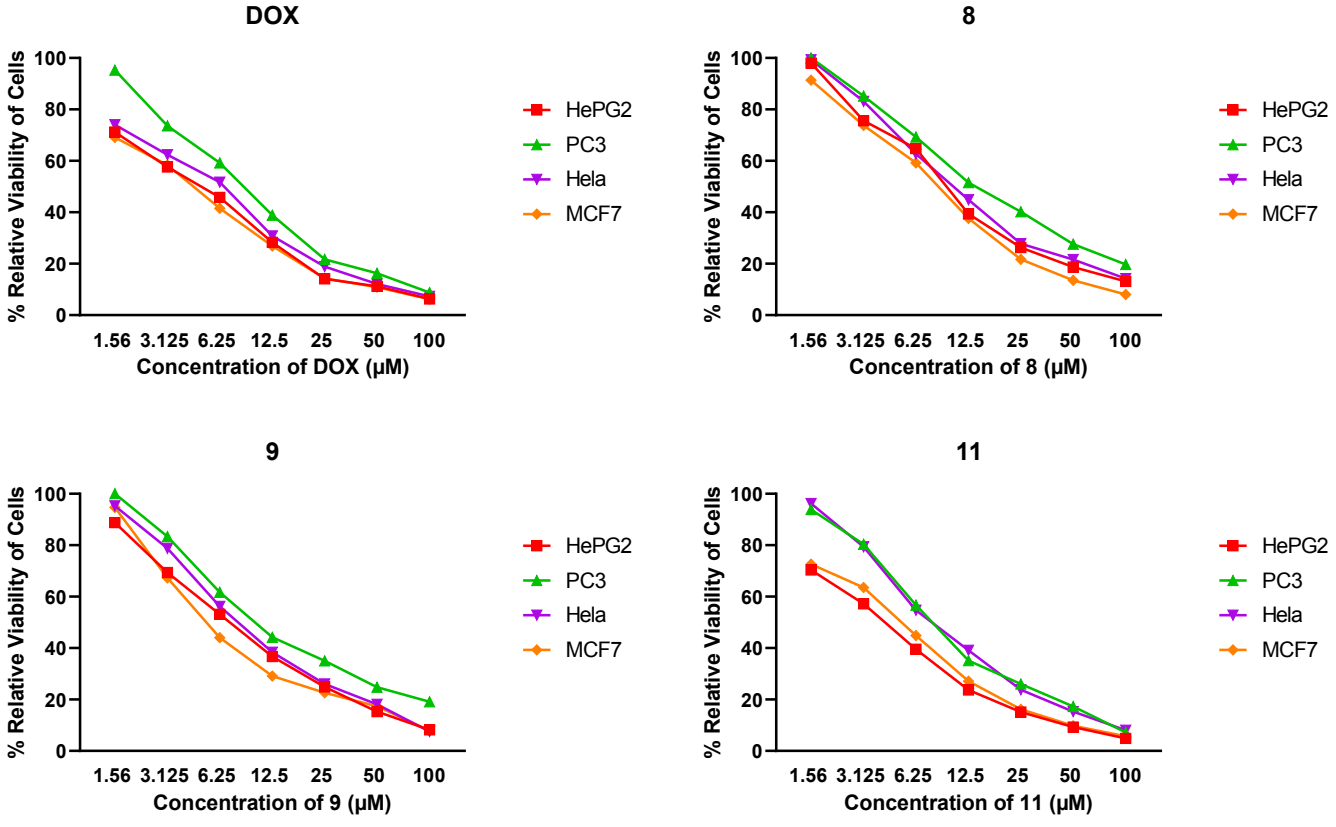

Fig 5. Relative viability of cells (%) against concentration of the newly synthesized compounds.

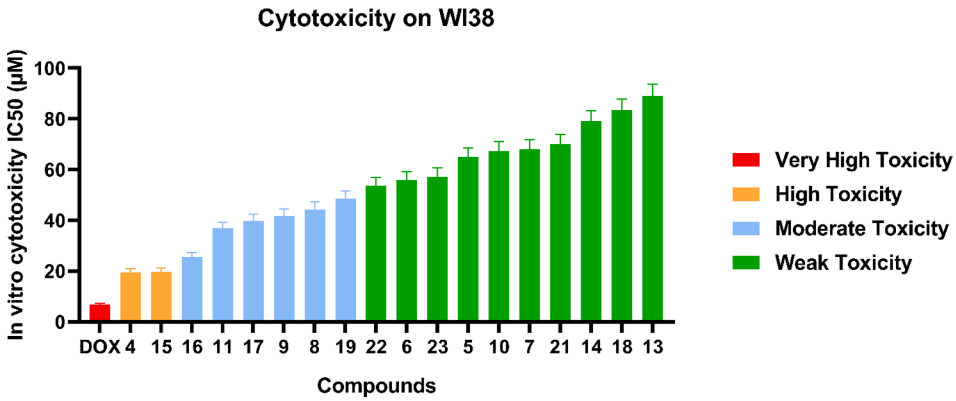

Fig 6. *In vitro* cytotoxicity (IC_{50}, μM) of the synthesized compounds against human normal cells (WI38). IC_{50}: compound concentration required to inhibit normal cell proliferation by 50% (Mean ± SD, n = 3). IC_{50} (μM). †1-10 (very high toxicity), *11–25 (high toxicity), 26–50 (moderate toxicity), 51–100 (weak toxicity), >100 (non-toxic) DOX: doxorubicin as a reference drug.

Table 2
IC_{50} values of compounds **8**, **9**, and **11** against PI3Kα.

Compound	Enzymatic IC_{50} (μM)
8	4.1 ± 0.2
9	7.8 ± 0.3
11	20.5 ± 0.7
LY294002	6.18 ± 0.2

Table 3
Effect of compound **8** and **9** on the cell cycle phases in MCF-7 cells.

Compound	Cell cycle distribution (%)				Comment
	G0-G1	S	G2/M	Pre-G1	
8	39.61	29.57	30.82	29.93	Pre-G1 apoptosis and cell growth arrest at G2/M
9	43.95	33.71	22.34	17.66	
Control MCF-7	53.89	36.26	9.85	1.78	

in Figures 8 and 9. Compounds **8** and **9** induced necrotic effect 9.36% and 6.29% 5.92% and 3.27% in MCF-7 at 24 h respectively compared to the control cells (1.21%).

Assessment of antimicrobial activity and antiquorum-sensing inhibitory activity

The antimicrobial activity of compounds **4**–**18** and **21**–**23** were evaluated against Gram-positive organisms (*Bacillus cereus* UW85 *and Staphylococcus aureus* ATCC 29213), Gram-negative isolates (*Escherichia coli* ATCC 12,435 and *Pseudomonas aeruginosa* PAO1) and fungi (*Candida albicans CS351)*. The screening was carried out following the two-fold serial dilution assay by using ampicillin as a reference antibacterial agent and fluconazole as a reference antifungal drug.[47] The results are summarized in Table 4. Diazotized aryl derivatives (Scheme 2) showed higher antimicrobial activity than other synthesized benzofuran derivatives.

For Gram-positive bacteria, compounds **13**, **14**, **15**, **16**, **17** and **18** showed good inhibition zone diameter in *Staphylococcus aureus* culture with 7, 9, 6, 7, 7 and 6 mm respectively in comparison to ampicillin (6 mm). Also, compounds **11**, **13**, **14**, **15**, **16** and **17** showed good inhibition zone diameter in *Bacillus cereus* culture with 11, 5, 6, 6, 8 and 6 mm

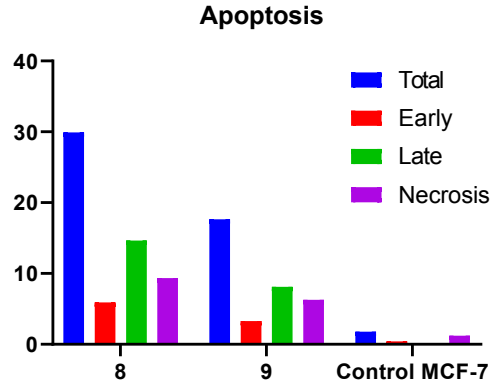

Fig 8. Effect of compound **8** and **9** on apoptosis and necrosis in MCF-7 cells.

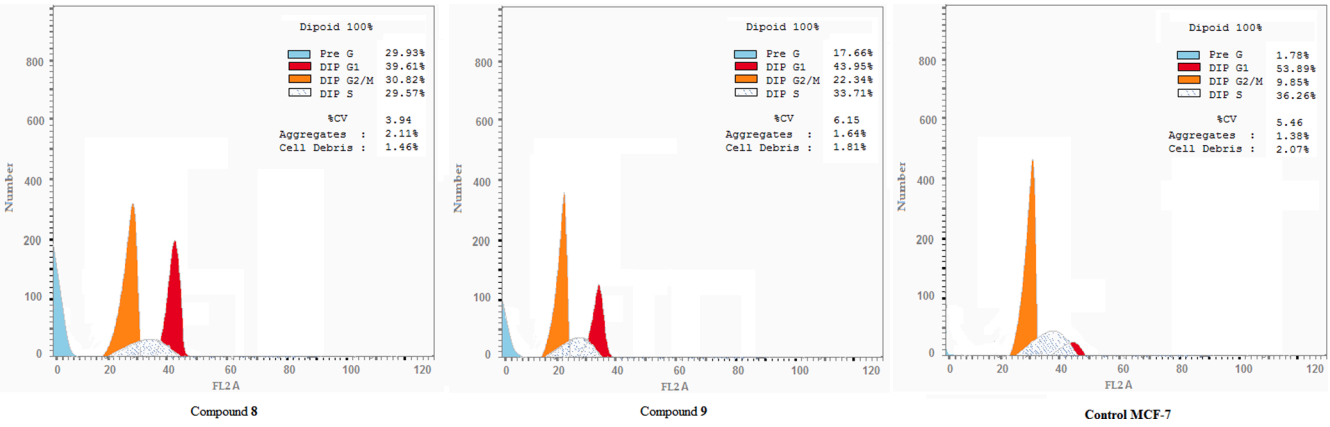

Fig 7. Effect of compounds **8** and **9** on the cell cycle distribution of MCF-7 cell line.

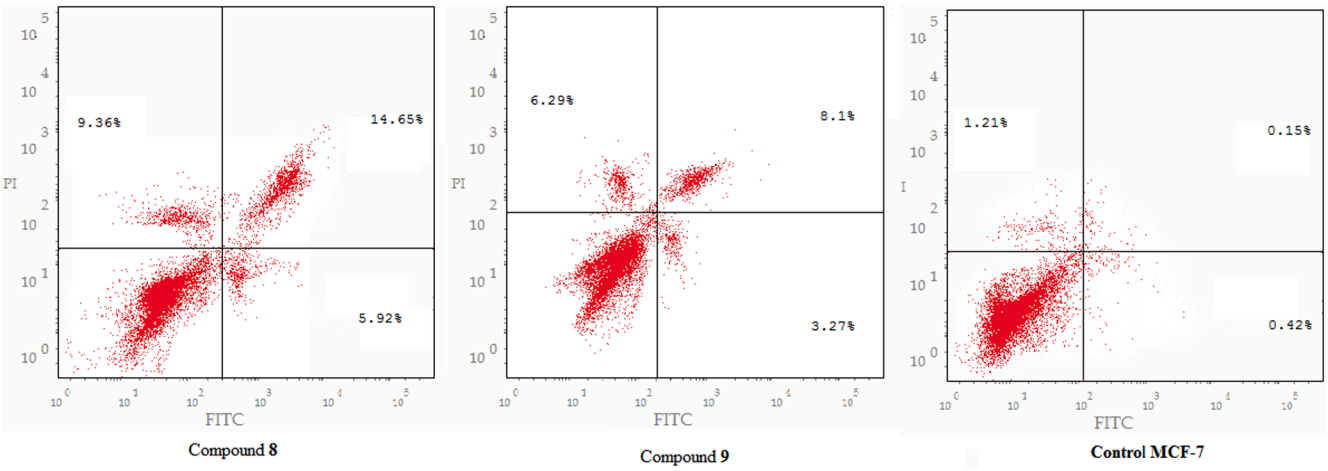

Fig 9. Apoptosis effect on MCF-7 cell line induced by compounds **8** and **9**.

Table 4
Antimicrobial and antiquorum-sensing activities of the synthesized compounds.

Compound No.	Inhibition zone diameter (mm)					QS inhibition (mm)
	Gram-positive bacteria		**Gram-negative bacteria**		**Fungi**	***Ch. Violaceum***
	S. aureus	***B. cereus***	***E. coli***	***P. aeruginosa***	***C. albicans***	
4	–	–	–	–	–	
5	–	–	–	–	–	
6	–	–	**–**	**–**	–	–
7	**–**	–	–	–	–	3
8	–	–	–	–	–	–
9	–	–	–	–	–	3
10	–	**–**	**–**	**–**	–	5
11	7	11	–	–	10	2
12	–	–	**–**	**–**	5	7
13	7	**5**	**–**	**–**	–	–
14	9	6	–	–	–	–
15	6	**6**	–	10	–	–
16	7	**8**	–	–	–	–
17	7	**6**	–	10	8	–
18	6	**–**	–	10	9	–
21	–	–	–	8	5	–
22	–	–	–	–	–	–
23	–	–	–	–	–	–
Ampicillin	6	10	10	–	–	NA
Fluconazole	NA	NA	NA	NA	8	NA

respectively in comparison to ampicillin (10 mm) (Table 4). By these observations, the benzofuran-aryl hydrazone hybrids show higher activity then other hybrids. Also, the activity against gram-positive bacteria significantly affected by the substitution of phenyl ring and it can be increased by *p*-Cl, *m*-CH_3, *o*-CH, *p*-CH_3 then *p*-NO_2 substitution.

For Gram-negative bacteria, compounds **15**, **17**, **18,** and **21** showed good inhibition zone diameter in *Pseudomonas aeruginosa* with 10, 10, 10 and 8 mm. (Table 4).

More importantly, compounds **11**, **12**, **17**, **18** and **21** showed good antifungal activity inhibition zone diameter in *Candida albicans* culture with 10, 5, 8, 9 and 5 mm respectively in comparison to fluconazole (8 mm) Table 4. Compounds **4**–**18** and **21**–**23** QS inhibitory activity were evaluated against *Ch. violaceum*. Compounds **7**, **9**, **10**, **11** and **12** exhibited QS inhibitory effect (Table 4). The summary of antimicrobial and antiquorum-sensing activities of the most active new compounds is shown in Chart 2 (created using BioRender).

2.7. Determination of minimal inhibitory concentrations (MICs)

The compounds that showed good inhibition zone diameter were subjected to MIC measuring to assess the lowest concentration of compound that inhibits microbial growth (MIC, μ g/mL). For Gram-positive bacteria, compounds **17**, *m*-Cl substituted, and **18**, *p*-NO3 substituted, have outstanding effectiveness towards *S. aureus* with value 8 μg/mL for both compounds in comparison to ampicillin (128 μg/mL). Also, compounds **11** and **16** showed potent efficacy towards *S. aureus* than ampicillin with 64 μg/mL. Furthermore, compounds **13**, **14** and **15** showed good activity towards *S. aureus* that similar to ampicillin with MIC equals 128 μg/mL. On behalf their efficacy towards *S. aureus*, compounds **11** and **16** showed good activity towards *B. cereus* with MIC equals 128 μg/mL and compounds **13**, **14**, **15** and **17** showed good activity with MIC equals 256 μg/mL (Table 5). For Gram-negative bacteria, compounds **15**, **17**, **18** and **21** showed good activity towards *P. aeruginosa* with MIC equals 512 μg/mL (Table 5). For antifungal activity, compound **11** showed potent efficacy than fluconazole (256 μg/mL) with 128 μg/mL. Moreover, compounds **12**, **18** and **21** showed good antifungal activity as fluconazole with MIC equals 256 μg/mL (Table 5). Finally, Compound **17** has outstanding efficacy towards *S. aureus, B. cereus, P. aeruginosa* and *C. albicans* (Table 5).

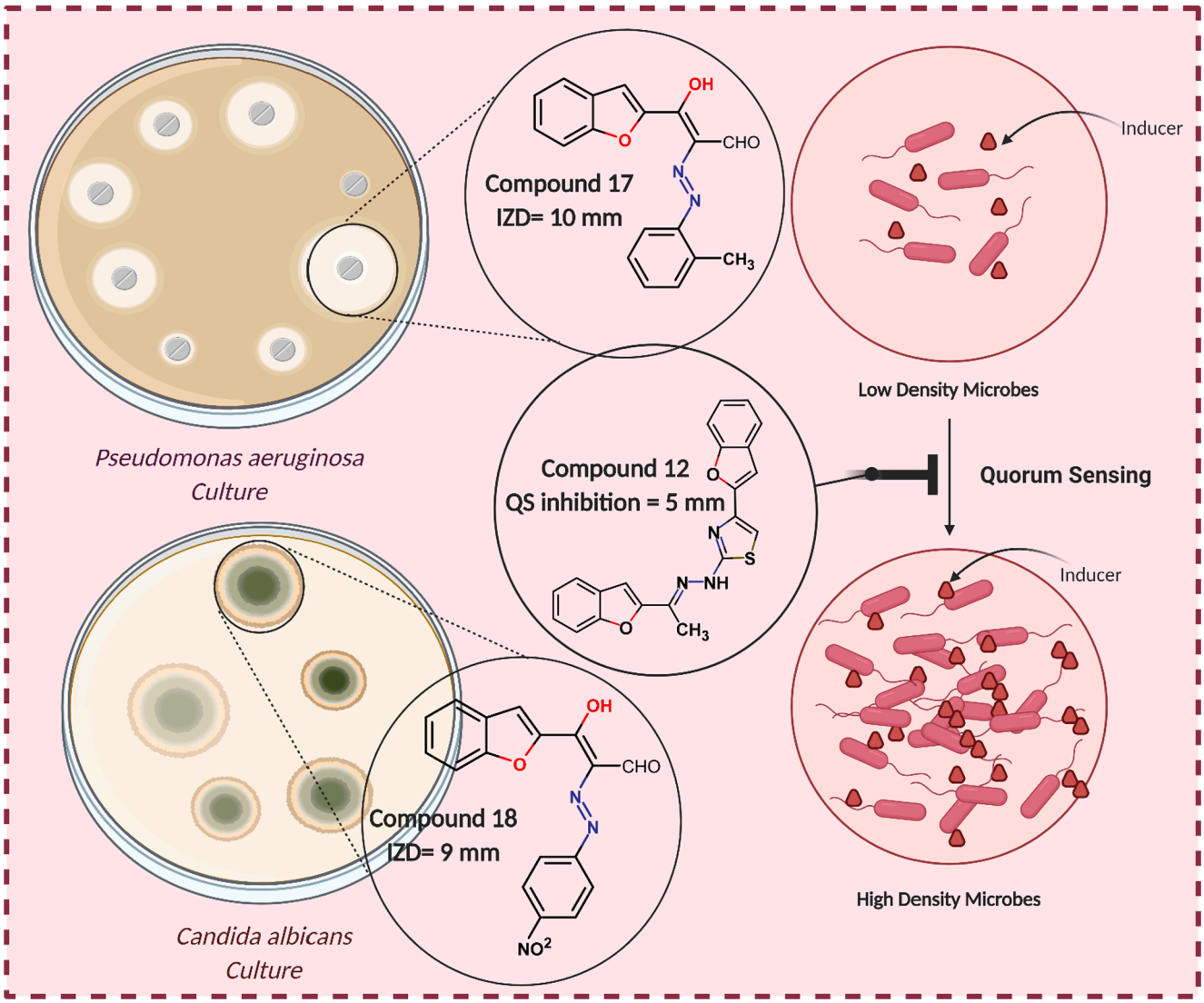

Chart 2. Summary of antimicrobial and antiquorum-sensing activities of the most active new compounds.

Table 5
A Minimal inhibitory concentration of the synthesized compounds.

Compound No.	Minimal inhibitory concentration (MIC; µg/mL)			
	S. aureus	*B. cereus*	*P. aeruginosa*	*C. albicans*
9	–	–	–	–
10	–	–	–	–
11	64	128	–	128
12	–	–	–	256
13	128	265	–	–
14	128	265	–	–
15	128	265	512	–
16	64	128	–	–
17	8	256	512	512
18	8	–	512	256
21	–	–	512	256
Ampicillin	128	128	>5000	–
Fluconazole	NA	NA	NA	256

2.8. Molecular modeling

2.8.1. Molecular docking study

In 2013, Furet *et al* published the co-crystal Structures of the PI3Kα and its interaction with Alpelisib.[48] Computational molecular modeling study was conducted to demonstrate the interaction between the synthesized compounds and PI3Kα using Molecular Operating Environment program (MOE). The docking study was conducted on compounds **8**, **9**, and **11** as the ligands, where the complex between PI3Kα and Alpelisib was selected as the docking model (PDB code: 4JPS).[48] Also, LY294002 tested for its interaction with PI3Kα as shown in Table 6.

In order to understand the mode of inhibition of PI3Kα by the newly synthesized compounds, molecular modeling was essentially required. A comparative modeling analysis between of the highly active compounds **8**, **9**, and **11** compared to Alpelisib and LY294002. Alpelisib demonstrated a strong binding through interaction with the hydrogen bond network including three water molecules and the Tyr836, Asp810, Asp933 and Lys802 side chains. Also, Lys802 residue made a hydrogen bond with one fluorine atom of the trifluoromethyl. Also, pair of donor–acceptor hydrogen bonds between amide group and residue of

Table 6
Docking interaction energy of compounds **8**, **9**, and **11** against PI3Kα.

Compound	Docking interaction energy (kcal/ mol)
8	−7.1
9	−6.4
11	−6.1
LY294002	−6.5
Alpelisib	−8.1

Gln859 and Val851 were showed (see Table 7).

Compound **8** showed a good fitting of the pocket and showed also pair of backbone donor between nitrogen and sulfur atoms and residue of Val851. The aligned conformation of compound **8** in binding site was aligned completely inside the pocket surface map explaining its activity experimentally (Fig. 10 (8b)). Compound **9** showed side chain acceptor with residue of Gln859, in addition to backbone donor with residue of Gln859. Compound **11** showed arene-H interaction and made with Arg770 and Gln859 two arene-cation and two arene-H interactions respectively Fig. 10.

2.8.2. Surface mapping

In additional confirmatory examination step to ensure the similarity between the most active compounds' binders to PI3K enzyme surface mapping study was performed for the conformers with the reference compound with interactions with pocket residue and with comparison with lowest energy. Fig. 11 showed nearly typical surface mapping contours of active compounds in interaction with selected enzyme. Therefore, that could be contributing to their good binding to our selected enzymes and put more evidence that their compounds anticancer activity may be due to PI3K inhibition (Fig. 12).

2.8.3. Contact preference

The purpose of the Contact Statistics application is to calculate from the 3D atomic coordinates of ligand preferred sites for hydrophobic and hydrophilic ligand atoms. Particularly, the purpose of this work was to study the interactions between the chemical components of the ligands and the protein microenvironment surrounding them. The results showed that the information underlying the fragment contacts is valuable as shows the similarity pattern of distribution of the hydrophobic and hydrophilic sites between our ligands **8**, **9**, **11**, and alpelisib (Fig. 13) and can also be exploited in understanding results of molecular docking simulations.

Better understanding of these moieties' interaction patterns can lead to better application of ligand-binding prediction, protein function recognition and drug design tools.

2.9. Physicochemical properties and Lipinski's rule of five

The most active synthesized compounds **8**, **9** and **11** were tested in order to verify compliance with the Lipinski rule of five relative to Alpelisib. Calculations were performed by SwissADME web service.[49] Predictions of ADME properties for the synthesized compounds are given in Table 7. The results found that the synthesized compounds comply with Lipinski's rule, similar to Alpelisib, suggesting that these compounds would possess drug-likeness characters. Predictions of water solubility of these compounds and Alpelisib found that all compounds have mostly similar solubility with Alpelisib, however, the topological polar surface area (TPSA) values for **8**, **9** and **1 l** are 78.66, 104.96 and 78.66, respectively, in comparison to Alpelisib (TPSA = 129) and potentially it may confer better gastrointestinal absorption for all compounds than Alpelisib, which marketed as oral tablets,.

3. Conclusion

A new benzofuran derivatives has been designed and synthesized. The structures of the synthesized compounds have been confirmed by the use of ^{1}H NMR, ^{13}C NMR. 2D ^{1}H–^{1}H NOESY NMR used to evaluate the structure of some compounds based on distance between atoms. The newly synthesized compounds was evaluated for their *in vitro* anticancer activity against HePG, MCF-7, Hela, and PC3 cell lines. Although, the safety index was assessed *in vitro* using WI38 cell line. Compounds **11**, **9**, and **8** showed the highest activity with an IC_{50} range of 4–8.99 μM, 6.55–13.14 μM and 8.49–16.72 μM respectively. PI3K was selected for evaluation as a target for the most active anticancer compounds **8**, **9** and **11**. Compound 8 showed the highest activity against PI3Kα inhibition with IC_{50} values 4.1. Also, compounds **9,** and **11** showed good inhibitory activity against PI3Kα with IC_{50} values 7.8, and 20.5 μM, respectively in comparison to 6.18 μM for compound LY294002. Molecular docking and binding affinity of the synthesized compounds were estimated and studied computationally using molecular operating environment software (MOE) as PI3Kα inhibitor. In addition, antimicrobial activity was evaluated against gram positive isolates as *Bacillus cereus* and *Staphylococcus aureus* gram negative isolate as *Escherichia coli* and *Pseudomonas aeruginosa* and *Candida albicans*. Compound **11**, **13**, **14**, **15**, **16**, and **17** showed higher activity than ampicillin against Gram positive organisms. Also, compounds **15**, **17**, **18** and **21** showed a good activity against Gram negative *Pseudomonas aeruginosa*. Although, Compounds **12**, **17**, and **21** showed antifungal activity higher than fluconazole. Also, Compound **17,** m-methyl substituted**,** has least MIC than other active compounds against *S. aureus*. Compound **11** showed better results than fluconazole against *C. albicans*. Compound **16** showed a better MIC than ampicillin against Gram positive organisms. In addition, the quorum sensing inhibiting effects were detected using *Chromobacterium violaceum*. Compounds **7**, **9**, **10**, **11**, and **12** showed better QS inhibitory activity.

4. Experimental

4.1. Chemistry

Melting points (°C) were recorded using a Stuart melting point apparatus and are uncorrected. IR spectra (KBr) were recorded on Thermo Fisher SCIENTIFIC Nicolet IS10. Spectrometer (ν in cm^{-1}) at Faculty of Pharmacy, Mansoura University. ^{1}H NMR and ^{13}C NMR spectra were obtained in BRUKER 400 MHz and BRUKER 600 MHz using TMS as internal standard (chemical shifts in ppm, δ units) at NMR unit, Faculty of Pharmacy, Mansoura University, Egypt and the NMR facility in the School of Medicine, University of Colorado, Denver, USA. Mass spectra were carried out on direct inlet part to mass analyzer in Thermo

Table 7
Solubility, topological surface area and calculated Lipinski's rule of five for compounds **8**, **9**, **1 l** and Alpelisib.

Comp.	Log *S*[a]	TPSA[b]	MW[c]	Mlog *P*[d]	nRB[e]	nHBA[f]	nHBD[g]	nVio[h]
8	−5.74	78.66	333.41	4.42	4	3	1	0
9	−4.49	104.96	343.40	3.27	7	5	1	0
11	−4.55	78.66	271.34	3.40	3	3	1	0
Alpelisib	−4.42	129	441.5	2.95	4	8	2	0

[a] Solubility parameter.
[b] Topological polar surface area (Å^2).
[c] Molecular weight (g/mol)
[d] Lipophilicity parameter.
[e] Number of rotatable bonds
[f] Number of hydrogen bond acceptors.
[g] Number of hydrogen bond donor.
[h] Number of violations to Lipinski's rule of five.

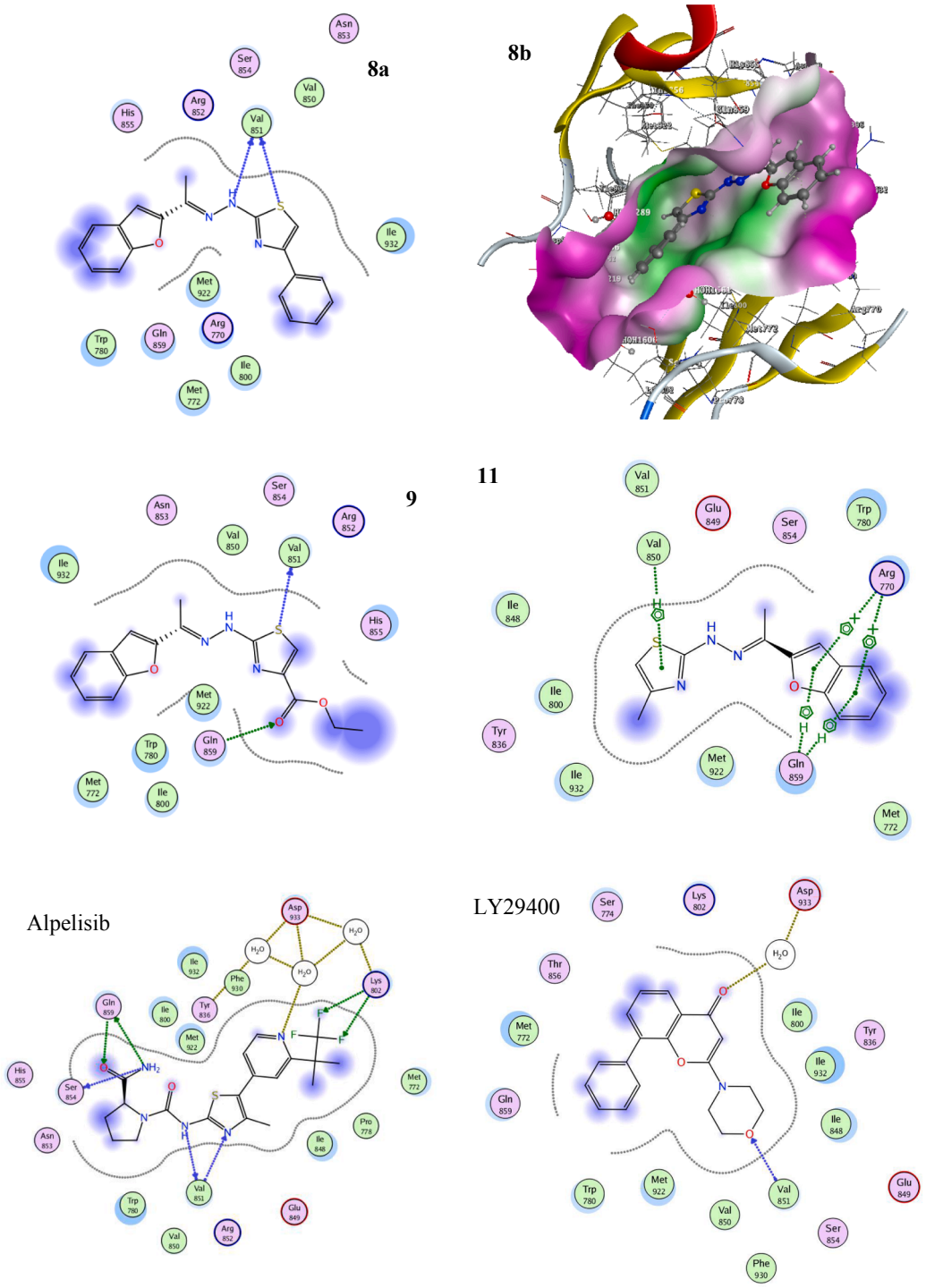

Fig 10. 2D binding mode and residues involved in the recognition of the most active compounds **8**, **9**, **11**, Alpelisib and LY294002 against PI3Kα 8b is the aligned conformation of compound **8** (ball and stick) occupying pocket (surface mapping).

Scientific GCMS model ISQ at the Regional Center for Mycology and Biotechnology (RCMB), Al-Azhar University, Egypt. The completion of reactions was monitored using thin layer chromatography (TLC) plates, Silica gel 60 F254 precoated (E. Merck) and the spots were visualized by UV (366 nm). All chemicals have been purchased from Sigma-Aldrich and used without further purification. Compounds **2**,[30] **3**,[31] **12**[36] and **20**[40] were prepared according to the literature.

4.1.1. General procedure for the preparation of compounds (4–11)

In 50 ml flask, to a solution of compound **3** (0.23 g, 1 mmol) in absolute ethanol (20 ml), appropriate α-halo ketone (1 mmol) was added to above solution and few drops of glacial acetic acid were added. The reaction mixture was refluxed for 24 h then partially concentrated under reduced pressure and left to cool. The separated solid product was filtered off and recrystallized from ethanol.

4.1.2. (E)-2-(2-(1-(benzofuran-2-yl)ethylidene)hydrazinyl)-4-(4-bromophenyl)thiazole (4).

Buff solid, mp = 254–256 °C, Yield = 70%. ^{1}H NMR (400 MHz, DMSO-d_6): δ = 7.85 (d, J = 7.8 Hz, 2H), 7.68 (d, J = 7.7 Hz, 1H), 7.63

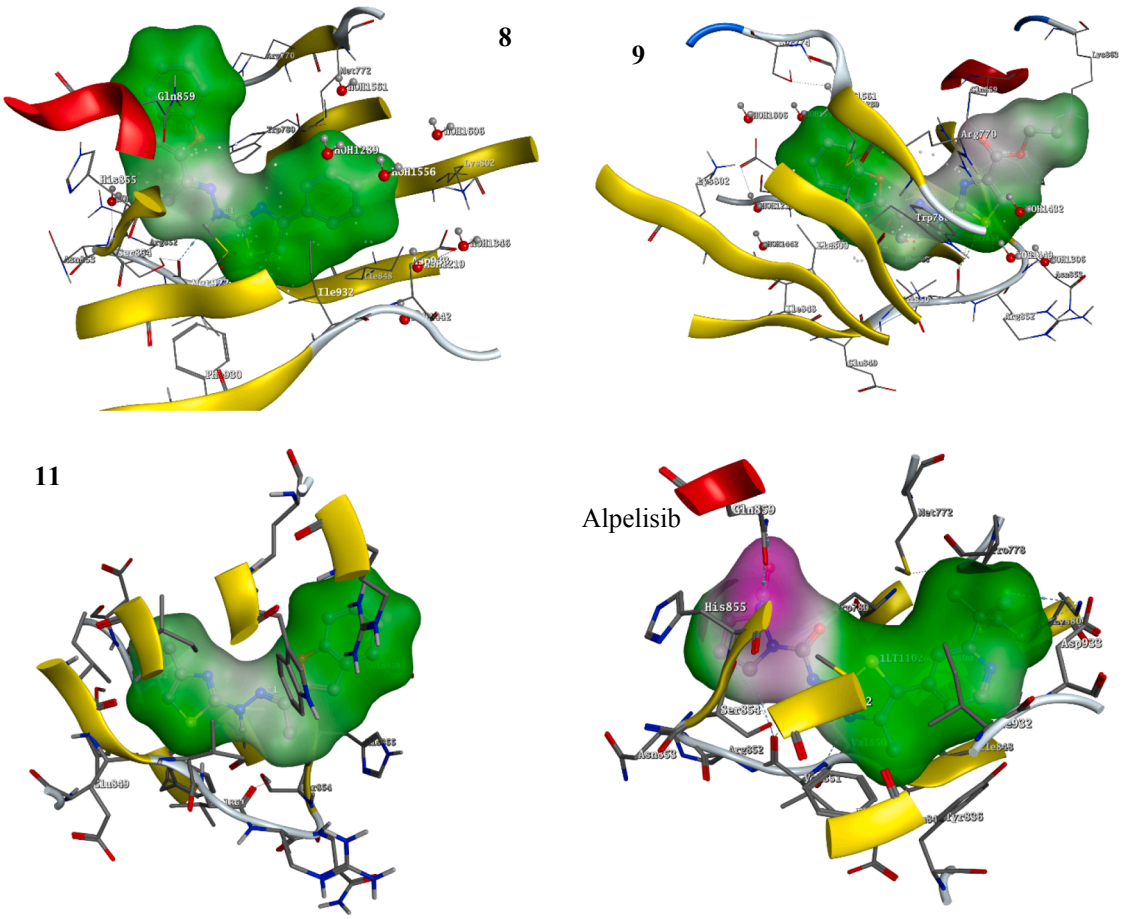

Fig 11. 3D surface map for compounds **8**, **9** and **11**. Pink: hydrophilic, white: neutral, green hydrophobic.

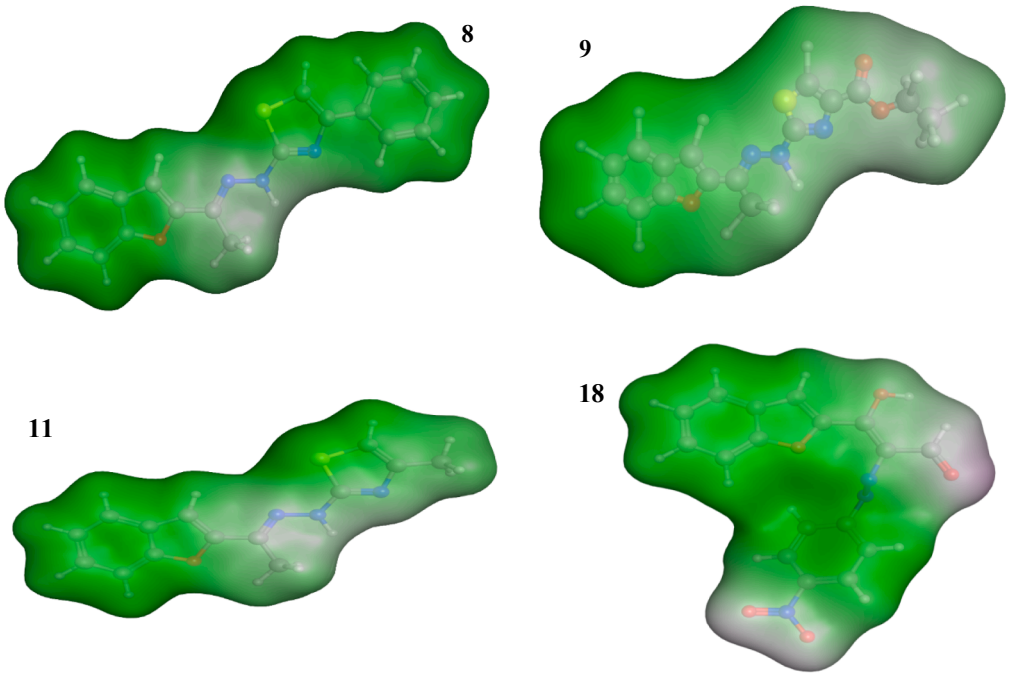

Fig 12. Surface map for compounds **8**, **9, 11** and **18**. Pink: hydrophilic, white: neutral, green hydrophobic.

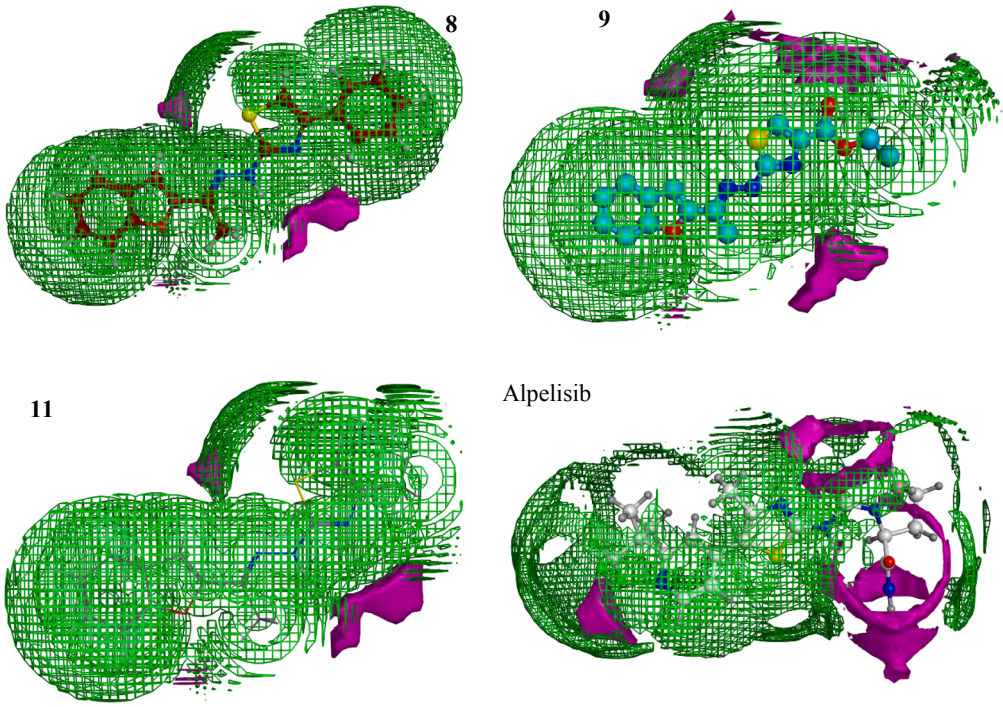

Fig 13. Contact statistics map for compounds **8**, **9**, **11,** and alpelisib (hydrophobic: green, hydrophilic: red). (For interpretation of the references to colour in this figure legend, the reader is referred to the web version of this article.)

(m, J = 6.4 Hz, 3H), 7.47 (s, 1H), 7.36 (t, J = 7.7 Hz, 1H), 7.32 (s, 1H), 7.28 (t, J = 7.4 Hz, 1H), 4.11 (s, exchangeable H), 2.36 (s, 3H). ^{13}C NMR (100 MHz, DMSO-d_6): δ = 155.06, 153.91, 131.87, 128.59, 126.04, 124.52, 124.17, 123.80, 122.05, 121.70, 111.73, 107.00, 14.36. MS *m/z* (%): 411.16 (M^+, 100), 413.17 (M^{+2}, 94.6). Elemental analysis for $C_{19}H_{14}BrN_3OS$, calculated C, 55.35; H, 3.42; Br, 19.38; N, 10.19; O, 3.88; S, 7.78. Found: C, 55.43; H, 3.53; Br, 19.49; N, 10.31; O, 3.48; S, 7.98.

4.1.3. *(E)-2-(2-(1-(benzofuran-2-yl)ethylidene)hydrazinyl)-4-(4-cholorophenyl)thiazole (5)*[50]

Yellow solid, mp = 248–250 °C, Yield = 73%. IR (KBr, cm^{-1}): 3229 (NH) 1640 (C═N). ^{1}H NMR (400 MHz, DMSO-d_6): δ = 7.91 (d, J = 8.2 Hz, 2H), 7.68 (d, J = 7.7 Hz, 1H), 7.64 (d, J = 8.2 Hz, 1H), 7.49 (d, J = 8.3 Hz, 2H), 7.45 (s, 1H), 7.36 (t, J = 7.7 Hz, 1H), 7.31 (s, 1H), 7.28 (t, J = 7.4 Hz, 1H), 3.81 (s, exchangeable H), 2.36 (s, 3H). ^{13}C NMR (100 MHz, DMSO-d_6): δ = 169.72, 154.98, 154.12, 138.92, 134.00, 132.42, 129.14, 128.64, 127.73, 125.89, 123.76, 121.98, 111.70, 106.56, 105.77, 14.30. MS *m/z* (%): 367.16 (M^+, 100), 369.12 (M^{+2}, 42.02). Elemental analysis for $C_{19}H_{14}ClN_3OS$, calculated: C, 62.04; H, 3.84; Cl, 9.64; N, 11.42; O, 4.35; S, 8.72. Found: C, 62.26; H, 3.95; Cl, 9.53; N, 11.53; O, 4.15; S, 8.83

4.1.4. *(E)-2-(2-(1-(benzofuran-2-yl)ethylidene)hydrazinyl)-4-(4-methylphenyl)thiazole (6)*

Orange solid, mp = 286–288 °C, Yield = 75%. ^{1}H NMR (400 MHz, DMSO-d_6): δ = 7.78 (d, J = 7.5 Hz, 2H), 7.68 (d, J = 7.6 Hz, 1H), 7.64 (d, J = 8.3 Hz, 1H), 7.36 (t, J = 7.5 Hz, 1H), 7.32 (s, 1H), 7.30 (s, 1H), 7.28 (s, 1H), 7.24 (d, J = 7.6 Hz, 2H), 4.12 (s, exchangeable H), 2.36 (s, 3H), 2.33 (s, 3H). ^{13}C NMR (100 MHz, DMSO-d_6): δ = 160.14, 155.84, 152.86, 145.16, 131.10, 130.30, 128.93, 128.08, 126.84, 124.34, 124.14, 123.13, 113.44, 112.30, 21.88, 15.83. Elemental analysis for $C_{20}H_{17}N_3OS$, calculated: C, 69.14; H, 4.93; N, 12.09; O, 4.61; S, 9.23. Found: C, 79.14; H, 4.83; N, 12.39; O, 4.11; S, 9.35.

4.1.5. *(E)-2-(2-(1-(benzofuran-2-yl)ethylidene)hydrazinyl)-4-(4-methoxyphenyl)thiazole (7)*

Pale pink solid, mp = 263–265 °C, Yield = 70%. ^{1}H NMR (400 MHz, DMSO-d_6): δ = 7.88 (d, J = 8.0 Hz, 2H), 7.74 (d, J = 7.7 Hz, 1H), 7.69 (d, J = 8.2 Hz, 1H), 7.42 (t, J = 7.7 Hz, 1H), 7.37 (s, 1H), 7.33 (t, J = 7.5 Hz, 1H), 7.26 (s, 1H), 7.05 (d, J = 7.8 Hz, 2H), 4.44 (s, exchangeable H), 3.85 (s, 3H), 2.42 (s, 3H). ^{13}C NMR (100 MHz, DMSO-d_6): δ = 159.30, 154.97, 154.19, 129.31, 128.66, 127.36, 125.85, 123.76, 121.96, 114.46, 114.33, 111.69, 106.45, 55.60, 14.29. ^{1}H–^{1}H-NOESY-2D-NMR (600 MHz, DMSO-d_6), 320 ms mixing time: cross peak 7.88 & 7.05 and between 7.6 & 6.94. Elemental analysis $C_{20}H_{17}N_3O_2S$, calculated: C, 66.10; H, 4.71; N, 11.56; O, 8.80; S, 8.82. Found: C, 66.25; H, 4.67; N, 11.26; O, 8.90; S, 8.94.

4.1.6. *(E)-2-(2-(1-(benzofuran-2-yl)ethylidene)hydrazinyl)-4-(4-phenyl)thiazole (8)*[51]

Buff solid, mp = 269–271 °C, Yield = 70%. ^{1}H NMR (600 MHz, DMSO-d_6): 7.89 (d, J = 7.8 Hz, 2H), 7.68 (d, J = 7.8 Hz, 1H), 7.63 (d, J = 7.8 Hz, 1H), 7.43 (t, J = 7.8 Hz, 2H), 7.38 (s, 1H), 7.35 (t, J = 7.8 Hz, 2H), 7.32 (s, 1H), 7.27 (t, J = 7.8 Hz, 2H), 2.37 (s, 3H). Elemental analysis for $C_{19}H_{15}N_3OS$, calculated C, 68.45; H, 4.53; N, 12.60; O, 4.80; S, 9.62. Found: C, 68.24; H, 4.75; N, 12.82; O, 4.60; S, 9.74.

4.1.7. *Ethyl (E)-2-(2-(2-(1-(benzofuran-2-yl)ethylidene)hydrazineyl) thiazol-4-yl)acetate (9)*

Yellow solid, mp = 198–200 °C, Yield = 75%. IR (KBr, cm^{-1}: 3451 (NH), 1725 (C═O). ^{1}H NMR (400 MHz, DMSO-d_6): δ = 7.70 (d, J = 7.5 Hz, 1H), 7.64 (d, J = 8.0 Hz, 1H), 7.43 (s, 1H), 7.39 (t, J = 7.7 Hz, 1H), 7.29 (t, J = 7.3 Hz, 1H), 6.83 (s, 1H), 4.47 (s, exchangeable H), 4.12 (q, J = 13.7, 6.7 Hz, 2H), 3.74 (s, 2H), 2.40 (s, 3H), 1.22 (t, J = 6.8 Hz, 3H). ^{13}C NMR (100 MHz, DMSO-d_6): δ = 169.91, 168.85, 155.01, 153.35, 128.47, 126.31, 123.89, 122.20, 111.81, 107.99, 107.77, 61.06, 56.49, 35.69 19.02, 14.92, 14.56. Elemental analysis for $C_{17}H_{17}N_3O_3S$, calculated: C, 59.46; H, 4.99; N, 12.24; O, 13.98; S, 9.34. Found: C, 59.65; H, 4.78; N, 12.35; O, 13.89; S, 9.48

4.1.8. (E)-2-(2-(1-(benzofuran-2-yl)ethylidene)hydrazineyl)-4-(benzofuran-5-yl)thiazole (10)

Brown solid, mp = 250–252 °C, Yield = 75%. ^{1}H NMR (400 MHz, DMSO-d_6): δ = 7.69 (d, J = 7.5 Hz, 2H), 7.63 (t, J = 9.2 Hz, 2H), 7.42 (s, 1H), 7.37 (s, 1H), 7.33 (d, J = 6.7 Hz, 2H), 7.28 (t, J = 7.2 Hz, 2H), 7.10 (s, 1H), 3.99 (s, exchangeable H), 2.37 (s, 3H). ^{13}C NMR (100 MHz, DMSO-d_6): δ = 170.31, 154.99, 154.53, 153.99, 153.64, 152.34, 139.33, 128.93, 128.54, 126.17, 125.99 125.18, 123.94, 122.12, 121.90, 111.71, 111.47, 107.51, 106.79, 102.72, 14.33. Elemental analysis for $C_{21}H_{15}N_3O_2S$, calculated: C, 67.54; H, 4.05; N, 11.25; O, 8.57; S, 8.59. Found: C, 67.34; H, 4.28; N, 11.57; O, 8.32; S, 8.67.

4.1.9. (E)-2-(2-(1-(benzofuran-2-yl)ethylidene)hydrazineyl)-4-methylthiazole (11)[51]

Brown solid, mp = 142–144 °C, Yield = 65%. ^{1}H NMR (400 MHz, DMSO-d_6): δ = 6.81 (d, J = 7.7 Hz, 1H), 6.74 – 6.69 (m, J = 9.4 Hz, 2H), 6.55 (t, J = 7.6 Hz, 1H), 6.45 (t, J = 7.6 Hz, 1H), 6.42 (s, 1H), 5.59 (s, exchangeable H), 1.72 (s, 3H), 1.56 (s, 3H). ^{13}C NMR (100 MHz, DMSO-d_6): δ = 155.17, 153.31, 128.42, 126.52, 123.98, 122.33, 111.88, 108.69, 104.60, 15.25, 15.12, 8.88. Elemental analysis for $C_{14}H_{13}N_3OS$, calculated: C, 61.97; H, 4.83; N, 15.49; O, 5.90; S, 11.82. Found: C, 61.77; H, 4.93; N, 15.59; O, 5.78; S, 11.96.

4.1.10. Synthesis of (E)-1-(benzofuran-2-yl)-3-(dimethylamino)prop-2-en-1-one (12)

Dimethylformamide dimethylacetal (DMFDMA) (0.12 g, 1 mmol) was added to solution of 2-acetyl benzofuran **(2)** (0.16 g, 1 mmol) in dry xylene (30 ml) the reaction mixture was refluxed upon completion of the reaction as judged by TLC. The mixture were concentrated under reduced pressure. The formed solid was filtered off, recrystallized from xylene to give the pure product golden yellow solid. mp = 129–131 °C, Yield = 90%. ^{1}H NMR (400 MHz, DMSO-d_6): δ = 7.81 (d, J = 12.4 Hz, 1H), 7.74 (d, J = 7.7 Hz, 1H), 7.66 (d, J = 8.3 Hz, 1H), 7.56 (s, 1H), 7.43 (t, J = 7.5 Hz, 1H), 7.30 (t, J = 7.5 Hz, 1H), 5.85 (d, J = 12.4 Hz, 1H), 3.17 (s, 3H), 2.94 (s, 3H). ^{13}C NMR (100 MHz, DMSO-d_6): δ = 176.56, 155.90, 154.84, 154.491, 128.04, 127.03, 123.91, 123.07, 112.29, 109.17, 91.47, 45.12, 37.70

4.1.11. General procedure for the preparation of (E)-3-(benzofuran-2-yl)-3-hydroxy-2-((E)- (substituted phenyl)diazenyl)acrylaldehyde compounds (13–18)

A cold solution of aryldiazonium chloride (1 mmol) was prepared by adding a solution of $NaNO_2$ (0.75 g, 20 mmol in 10 ml H_2O) to a cold solution of appropriate aniline derivative (1 mmol) in concentrated HCl (5 ml) with stirring. The resulting solution of the aryldiazonium salt was then added to a cold solution of Compound **16** in EtOH (50 ml) containing sodium acetate (0.14 g, 1 mmol). The mixture was stirred at room temperature for 1 h and the solid product formed was collected by filtration and crystallized from ethanol.

4.1.12. (E)-3-(benzofuran-2-yl)-3-hydroxy-2-((E)-(4-methoxyphenyl) diazenyl)acrylaldehyde (13)

Dark brown solid. mp = 137–139 °C, Yield = 80%. ^{1}H NMR (400 MHz, DMSO-d_6): δ = 14.17 (s, exchangeable H), 9.98 (s, 1H), 7.91 (m, 2H), 7.76 (d, J = 8.3 Hz, 1H), 7.62 – 7.52 (m, 1H), 7.48 – 7.33 (m, J = 7.4 Hz, 2H), 7.27 (s, 2H), 6.84 (m, 1H), 3.79 (s, 3H). ^{13}C NMR (100 MHz, DMSO-d_6): δ = 187.95, 163.62, 160.78, 155.30, 154.16, 153.09, 150.76, 143.34, 131.14, 130.39, 129.33, 128.15, 124.40, 117.59, 113.08, 112.78, 109.96, 102.57, 55.64. Elemental analysis for $C_{18}H_{14}N_2O_4$, calculated: C, 67.07; H, 4.38; N, 8.69; O, 19.86. Found: C, 67.25; H, 4.16; N, 8.87; O, 19.68.

4.1.13. (E)-3-(benzofuran-2-yl)-3-hydroxy-2-((E)-(4-cholorophenyl) diazenyl)acrylaldehyde (14)

Dark brown solid, mp = 165–167 °C, Yield = 85%. ^{1}H NMR (400 MHz, DMSO-d_6): δ = 14.26 (s, exchangeable H), 9.97 (s, 1H), 7.93 (d, J = 6.9 Hz, 1H), 7.89 (d, J = 4.6 Hz, 1H), 7.76 (d, J = 8.3 Hz, 1H), 7.70 (d, J = 8.8 Hz, 2H), 7.55 (m, 2H), 7.46 (m, 1H), 7.39 (t, J = 7.5 Hz, 1H). ^{13}C NMR (100 MHz, DMSO-d_6): δ = 188.02, 178.79, 155.34, 150.68, 141.01, 132.71, 130.52, 130.12, 129.81, 128.83, 127.54, 124.48, 124.39, 119.34, 117.75, 117.56, 112.52. MS m/z (%): 326.25 (M^+, 49.32), 328.26 (M^{+2}, 19.91). Elemental analysis for $C_{17}H_{11}ClN_2O_3$, calculated: C, 62.49; H, 3.39; Cl, 10.85; N, 8.57; O, 14.69. Found: C, 62.27; H, 3.57; Cl, 10.77; N, 8.33; O, 14.57.

4.1.14. (E)-3-(benzofuran-2-yl)-3-hydroxy-2-((E)-(4-methylphenyl) diazenyl)acrylaldehyde (15)[52]

Dark brown solid, mp = 146–148 °C, Yield = 75%. ^{1}H NMR (400 MHz, DMSO-d_6): δ = 14.46 (s, exchangeable H), 9.97 (s, 1H), 7.92 (d, J = 7.7 Hz, 1H), 7.89 (s, 1H), 7.76 (d, J = 8.4 Hz, 1H), 7.59 – 7.52 (m, 3H), 7.39 (dd, J = 14.5, 7.2 Hz, 1H), 7.30 (d, J = 8.3 Hz, 2H), 2.33 (s, 3H). ^{13}C NMR (100 MHz, DMSO-d_6): δ = 187.82, 178.67, 155.25, 150.72, 139.51, 136.57, 132.19, 130.73, 130.36, 128.72, 127.56, 124.41, 124.36, 117.69, 117.45, 116.23, 112.47, 21.06. Elemental analysis for $C_{18}H_{14}N_2O_3$, calculated: C, 70.58; H, 4.61; N, 9.15; O, 15.67. Found: C, 70.36; H, 4.83; N, 9.25; O, 15.47

4.1.15. (E)-3-(benzofuran-2-yl)-3-hydroxy-2-((E)-(3-methylphenyl) diazenyl)acrylaldehyde (16)

Light orange solid, mp = 115–117 °C, Yield = 75%. ^{1}H NMR (400 MHz, DMSO-d_6): δ = 14.38 (s, exchangeable H), 9.98 (s, 1H), 7.96 – 7.88 (m, 2H), 7.76 (d, J = 8.2 Hz, 1H), 7.56 (t, J = 7.6 Hz, 1H), 7.48 (d, J = 8.2 Hz, 2H), 7.43 – 7.33 (m, 2H), 7.10 (d, J = 7.3 Hz, 1H), 2.36 (s, 3H). ^{13}C NMR (100 MHz, DMSO-d_6): δ = 188.67, 178.53, 155.31, 150.56, 139.49, 133.28, 131.72, 128.83, 128.39, 127.57, 126.85, 126.61, 124.51, 124.39, 117.67, 115.82, 112.50, 16.84. Elemental analysis for $C_{18}H_{14}N_2O_3$, calculated: C, 70.58; H, 4.61; N, 9.15; O, 15.67. Found: C, 70.36; H, 4.83; N, 9.25; O, 15.57.

4.1.16. (E)-3-(benzofuran-2-yl)-3-hydroxy-2-((E)-(2-methylphenyl) diazenyl)acrylaldehyde (17)

Light orange solid, mp = 131–133 °C, Yield = 75%. ^{1}H NMR (400 MHz, DMSO-d_6): δ = 14.78 (s, exchangeable H), 10.02 (s, 1H), 7.97 (s, 1H), 7.94 (d, J = 7.8 Hz, 1H), 7.82 – 7.74 (m, 2H), 7.57 (t, J = 7.4 Hz, 1H), 7.45 – 7.34 (m, 3H), 7.23 (t, J = 7.3 Hz, 1H), 2.42 (s, 3H). ^{13}C NMR (100 MHz, DMSO-d_6): δ = 188.43, 178.88, 155.52, 150.61, 147.68, 147.57, 134.17, 129.09, 127.52, 126.08, 124.64, 124.49, 119.77, 118.34, 117.72, 115.60, 112.62. Elemental analysis for $C_{18}H_{14}N_2O_3$, calculated: C, 70.58; H, 4.61; N, 9.15; O, 15.67. Found: C, 70.46; H, 4.83; N, 9.25; O, 15.57.

4.1.17. (E)-3-(benzofuran-2-yl)-3-hydroxy-2-((E)-(4-nitrolphenyl) diazenyl)acrylaldehyde (18)

Dark brown solid. mp = 220–222 °C, Yield = 80%. ^{1}H NMR (400 MHz, DMSO-d_6): δ = 9.99 (s, exchangeable H), 9.65 (s, 1H), 8.34 (d, J = 9.0 Hz, 1H), 8.27 (d, J = 9.0 Hz, 1H), 8.02 (s, 1H), 7.95 (d, J = 9.6 Hz, 1H), 7.87 (d, J = 8.9 Hz, 2H), 7.80 (d, J = 8.2 Hz, 1H), 7.59 (d, J = 7.4 Hz, 1H), 7.41 (t, J = 7.3 Hz, 1H). ^{13}C NMR (100 MHz, DMSO-d_6): δ = 188.43, 147.68, 144.42, 134.17, 130.41, 129.09, 127.52, 126.08, 124.64, 124.49, 119.77, 118.34, 117.72, 115.60, 112.93, 112.62. Elemental analysis for $C_{17}H_{11}N_3O_5$, calculated: C, 60.54; H, 3.29; N, 12.46; O, 23.72. Found: C, 60.33; H, 3.47; N, 12.26; O, 23.96

4.1.18. Synthesis of 2-(benzofuran-2-yl)-1-(4-methylpiperazin-1-yl) ethanethione (19)

A mixture of 2-acetyl benzofuran **(2)** (0.16 g, 1 mmol) and S_8 (10 mmol) was stirring in glycerol/K_2CO_3 (10:1, 25 ml) for at 80℃ for 2 h. The reaction mixture purred in ice/water then the product extracted by ethyl acetate and purified with column chromatography (ethyl acetate: petroleum ether, 2:1) to give compound **19**.

Brown solid, mp = 119–121 °C, Yield = 70%. ^{1}H NMR (400 MHz, $CDCl_3$): δ = 7.93 (s, 1H), 7.89 (d, J = 7.8 Hz, 1H), 7.78 (d, J = 8.4 Hz,

1H), 7.61 (t, $J = 7.7$ Hz, 1H), 7.42 (t, $J = 7.5$ Hz, 1H), 4.23 (s, 2H), 3.67 (s, 2H), 3.38 (s, 2H) 2.61 – 2.55 (m, 2H), 2.52 (s, 2H) 2.41 – 2.35 (m, 2H), 2.25 (s, 3H). ^{13}C NMR (100 MHz, $CDCl_3$): δ = 191.83, 177.36, 156.16, 149.74, 129.90, 127.11, 124.96, 124.61, 118.42, 112.88, 54.75, 53.91, 51.87, 47.26, 45.49. Elemental analysis for $C_{15}H_{18}N_2OS$, calculated: C, 65.66; H, 6.61; N, 10.21; O, 5.83; S, 11.69. Found: C, 65.86; H, 6.41; N, 10.11; O, 5.76; S, 11.87.

4.1.19. Synthesis of 2-(4-methoxyphenyl)-2-oxoethyl (E)-2-(1-(benzofuran-2-yl)ethylidene)hydrazine-1-carbodithioate (21)

In 50 ml flask, to a solution of compound **20** (0.17 g, 1 mmol) in dry DMF (20 ml), carbon disulfide (0.38 g, 5 mmol) was added. The reaction mixture was stirring for 10 min then adding sodium phosphate (10 mmol) for 3hr followed by addition of 4-methoxyphenacyl bromide (0.23 g, 1 mmol) and stirring to the end of reaction judging with TLC. The separated solid product was filtered off to give compound **21**.

Light brown solid, mp = 88–90 °C, Yield = 70%. 1H NMR (400 MHz, DMSO-d_6): δ = 12.65 (s, exchangeable H), 8.07 (d, $J = 8.7$ Hz, 2H), 7.95 (s, 1H), 7.73 (d, $J = 7.7$ Hz, 1H), 7.66 (d, $J = 8.3$ Hz, 1H), 7.55 (s, 1H), 7.41 (t, $J = 7.8$ Hz, 1H), 7.30 (t, $J = 7.5$ Hz, 1H), 7.09 (d, $J = 8.7$ Hz, 2H), 4.86 (s, 1H), 3.86 (s, 2H), 2.88 (s, 3H), 2.43 (s, 3H). 13C NMR (100 MHz, DMSO-d_6): δ = 198.70, 192.26, 163.78, 162.87, 155.32, 153.17, 144.10, 131.08, 129.57, 128.29, 126.89, 124.01, 122.49, 114.44, 111.94, 110.02, 56.03, 36.28, 31.24, 14.90. Elemental analysis for $C_{20}H_{18}N_2O_3S_2$, calculated: C, 60.28; H, 4.55; N, 7.03; O, 12.04; S, 16.09. Found: C, 60.36; H, 4.35; N, 7.15; O, 12.14; S, 16.19.

4.1.20. General procedure for the preparation of compounds (22–23)

A mixture of compound 20 (10 mmol) and appropriate benzaldehyde derivative (10 mmol) was refluxed in ethanol/acetic acid (24:1, 25 ml) for 3 h. The excess of solvent was then removed under reduced pressure, the precipitate formed after cooling was collected by filtration and recrystallized from ethanol to give the corresponding compound.

4.1.21. (E)-1-(1-(benzofuran-2-yl)ethylidene)-2-((E)-4-nitrobenzylidene) hydrazine (22)

Yellow solid, mp = 180–182 °C, Yield = 80%. IR (KBr, cm–1): 1531 & 1351 (NO_2). ^{1}H NMR (400 MHz, DMSO-d_6): δ = 8.91 (s, 1H), 8.70 (s, 1H), 8.36 (d, $J = 8.1$ Hz, 1H), 8.31 (d, $J = 7.7$ Hz, 1H), 7.81 (t, $J = 7.9$ Hz, 1H), 7.74 (d, $J = 7.7$ Hz, 1H), 7.68 (d, $J = 8.3$ Hz, 1H), 7.57 (s, 1H), 7.42 (t, $J = 7.7$ Hz, 1H), 7.31 (t, $J = 7.5$ Hz, 1H), 2.36 (s, 3H). ^{13}C NMR (100 MHz, DMSO-d_6): δ = 161.01, 155.25, 153.82, 151.58, 148.66, 135.68, 134.92, 131.14, 128.23, 126.85, 126.32, 123.97, 123.12, 122.56, 122.01, 109.68, 14.97. Elemental analysis for $C_{17}H_{13}N_3O_3$, calculated: C, 66.44; H, 4.26; N, 13.67; O, 15.62. Found: C, 66.26; H, 4.48; N, 13.57; O, 15.72.

4.1.22. (E)-1-(1-(benzofuran-2-yl)ethylidene)-2-((E)-3-chlorobenzylidene)hydrazine (23)

Yellow powder, mp = 144–146 °C, Yield = 85%. ^{1}H NMR (400 MHz, DMSO-d_6): δ = 8.94 (s, 1H), 8.73 (s, 1H), 8.38 (d, $J = 8.1$ Hz, 1H), 8.33 (d, $J = 7.7$ Hz, 1H), 7.83 (t, $J = 7.9$ Hz, 1H), 7.75 (d, $J = 7.7$ Hz, 1H), 7.69 (d, $J = 8.2$ Hz, 1H), 7.59 (s, 1H), 7.43 (t, $J = 7.6$ Hz, 1H), 7.31 (d, $J = 7.4$ Hz, 1H), 2.37 (s, 3H). ^{13}C NMR (100 MHz, DMSO-d_6): δ = 161.04, 155.27, 153.84, 153.54, 148.71, 135.71, 134.94, 131.18, 128.25, 126.87, 126.36, 124.00, 123.17, 122.57, 112.04, 109.71, 14.99. Elemental analysis for $C_{17}H_{13}ClN_2O$, calculated: C, 68.81; H, 4.42; Cl, 11.95; N, 9.44; O, 5.39. Found: C, 68.61; H, 4.24; Cl, 11.77; N, 9.26; O, 5.29

4.2. Antitumor screening and using MTT assay in vitro cytotoxicity against human normal cells

All the newly synthesized compounds were evaluated against human cancer cell lines using doxorubicin (DOX) as reference drug. The panel consisted of Hepatocellular carcinoma (HePG2), Mammary gland Breast cancer (MCF-7), Epitheliod Carcinoma Cervix cancer (Hela) and Human prostate cancer (PC3). Human lung fibroblast (WI38) was used to assay the cytotoxicity effect on normal cell. The cell line was obtained from ATCC via Holding company for biological products and vaccines (VACSERA), Cairo, Egypt. The cytotoxic activity was defined as the concentration of the compound that causes 50% growth inhibition compared with the growth of untreated cells.

4.3. Human PI3K enzyme inhibition assay

PI3K activity was verified by enzyme-linked immunosorbent assay (ELISA) assay technique. The assay exploited a specific antibody for human PI3K firmly coated on a 96-well plate, in which 100 ml of the standard solution or the tested compounds were added to every well at room temperature. Then, the mean absorbance of each group of standard and tested compounds was determined. The standard curve was drawn on log–log paper with the absorbance on the Y-axis and the standard concentration on the X-axis. Percent Inhibition was assessed through comparing both test compounds and control results, whereas IC_{50} was assessed from concentration/inhibition curve using LY294002 as a standard.

4.4. Cell cycle arrest analysis and apoptosis detection

Apoptosis detection was performed by using Annexin V-FITC and PI apoptosis kit (eBioscienceTM, San Diego, CA, USA). Mcf cells were plated at a 600,000 cells/mL density onto a six well plate. After 24 h of incubation, the cells were treated with compound 15 at 10 Mg/mL. Cells grown in media containing an equivalent amount of DMSO served as the solvent control. After 24 h, the cells were stained with an Annexin V-FITC conjugate and propidium iodide (PI), and the percentage of apoptotic, necrotic, and living cells was determined according to the protocol provided by the Annexin V-FITC and PI apoptosis kit. The cells' emitted fluorescence was analyzed by flow cytometry (NovoCyte, ACEA Biosciences Inc, San Diego, CA, US) through the NovoExpress 1.3.0 software (ACEA Biosciences Inc, San Diego, CA, US), acquiring 1 × 104 events per sample using the population plot "dot plot", where each point corresponds to a single event with a specific fluorescence signal in reference to the axes; Annexin V-FITC green fluorescence in abscissa vs. PE red fluorescence in ordinate.

4.5. Microbes and culture media

In this research the antimicrobial effects of different compounds against Gram positive organisms such as *Bacillus cereus* UW85, *Staphylococcus aureus* ATCC 29,213 and against Gram negative isolates including *Escherichia coli* ATCC 12435, *Pseudomonas aeruginosa* PAO1. Furthermore, the antifungal potential of the compound was evaluated against *Candida albicans* CS351. In addition, the quorum sensing inhibiting effects were detected using *Chromobacterium violaceum* ATCC 12,472 (kindly provided from Prof. Bob Mclean, Department of Biology, Texas State University, USA). The bacterial strains used in this study were grown in Luriae Bertani (LB) media (1% tryptone, 0.5% yeast extract (Bacto-agar, BD Difco), and 1.0% NaCl solidified with 1.5% agar). Muller Hinton media was used for the assay of antibacterial studies and Sabouraud's media (BD Difco) was used for antifungal activity. Ampicillin/ clavulanic acid (EPICO Company) and fluconazole (Pfizer Company) were used as antibacterial and antifungal standards, respectively.

4.6. Assessment of antimicrobial activity

Antibacterial effect of the newly synthesized compounds was performed using agar plate diffusion method. The overnight culture of both Gram-positive and Gram-negative isolates in Muller Hinton (MH) broth was diluted to 0.5 McFarland. The Muller Hinton (MH) agar at 50 °C was

inoculated with 20 μL of the diluted cultures, mixed and poured into 9-cm-diameter sterile plates and solidify. Sterile cork borer was used to make cups into the solidified plates and the agar in the cups were removed. The tested compounds were dissolved in DMSO to get a final concentration of 5 mg/mL. One hundred microliter of each compound was added to each cup and DMSO was added as a negative control. The plates were incubated at 37 °C for 24 h in to assess the antibacterial and antifungal activities. The diameter of inhibition zone was measured in millimeter and the activity of the tested compounds was estimated in comparison to ampicillin/ clavulanic and fluconazole as reference antibacterial and antifungal drugs

4.7. Quorum-sensing inhibitory activity

C. violaceum ATCC 12,472 was propagated in Luria-Bertani broth media for at 28 °C 48 h. Luria-Bertani agar plates were prepared and left to complete solidification, *C. violaceum* was inoculated (50 μL/plate) in 5 ml soft LB agar and poured as a top layer to the solidified LB plates. Cups were made in the plates and 100 μL of the synthesized compound dissolved in DMSO (5 mg/ml) compounds was added to each well and DMSO was also included as negative controls. The growth of the *C. violaceum* was allowed at 28 °C for 48 h, *C. violaceum* growth recognized as a bacterial loan with violet pigment. The compound possessing antimicrobial effects would result in a clear inhibition zone around the cup, with radius (r1 mm). Compounds exhibiting quorum sensing inhibiting potential was detected as inhibition of the violet pigment around the wells. Both growth and pigment inhibition were measured as radius (r2 mm). Hence, the QS inhibition was determined by subtracting bacterial growth inhibition (r1) from the total radius (r2); thus, QS inhibition = (r2 − r1) in mm.[53,54]

4.8. Determination of minimal inhibitory concentrations (MICs)

The compound exhibited antimicrobial activities as indicated by agar diffusion method were selected and evaluated for antibacterial effects according to the CLSI, 2015 and for antifungal effects according the standard methods *CLSI M27-A3* and *CLSI M38-A2* (CLSI 2008). Dilutions of the selected compounds were prepared 1:1 in 0.1 ml MH broth to study their antibacterial effects and yeast peptone dextrose for antifungal activity. Each well was inoculated with 0.01 of the diluted bacterial suspension (5×10^6 CFU/ml). The antibacterial activity of ampicillin/clavulanic and fluconazole was estimated and used as a positive control. The microtiter plates were incubated at 37 °C for 18 h. The minimal inhibitory concentration was detected to the lowest concentration that inhibited visible microbial growth

4.9. Molecular modeling

The three-dimensional structures of some selected substituted benzofuran **8**, **9**, and **11** which represent the best anticancer activity, in their neutral forms, were built by using the MOE of Chemical Computing Group Inc. software 2014. The Lowest energy conformers of new analogues 'global-minima' was docked into the binding pocket of model 4JPS PDB.[48] It was obtained from the Protein Data Bank of Brookhaven National Laboratory. The hydrogens were added, then enzyme structure was subjected a refinement protocol where the constraints on the enzyme were gradually removed and minimized until the RMSD gradient was 0.01 kcal/mol Å. Energy minimization was performed using the molecular mechanics force field 'AMBER.' For each benzofuran derivative, energy minimizations (EM) were performed using 1000 steps of steepest descent, followed by conjugate gradient minimization to a RMSD energy gradient of 0.01 Kcal/mol Å. The active site of the enzyme was detected in reference compound pdb file. The compounds under study underwent flexible alignment experiment using 'Molecular Operating Environment' software (MOE of Chemical Computing Group Inc., on a Core i5 2.40 GHz workstation). The molecules were constructed using the Builder module of MOE. Their geometry was optimized by using the MMFF94 force field followed by a flexible alignment using systematic conformational search. The Lowest energy aligned conformers were identified. For each analogue, the partial atomic charges were assigned using the semi-empirical mechanical calculation "AM1"method implemented in the program. Conformational search was done. All the conformers were minimized until the RMSD deviation was 0.01 Kcal/mol, then subjected to surface mapping, color coded: pink, hydrogen bond; white: neutral; green hydrophobic.

4.10. Physicochemical properties and Lipinski's rule of five

Lipophilicity "log P" and the Polar surface area (Å2) "TPSA" for the tested analogues were estimated using SWISS ADME web service.

Declaration of Competing Interest

None.

Acknowledgments

We would like to thank NMR unit, Faculty of Pharmacy, Mansoura University and its manager Prof. Dr. Dr. Hussein I. El-Subbagh for his great efforts for conducting all NMR analysis of this work. Also, we are grateful for Professor Beat Vögeli, University of Colorado, Denver, USA for his support. We Thanks Mansoura University, Egypt for the financial support.

Appendix A. Supplementary material

Supplementary data to this article can be found online at https://doi.org/10.1016/j.bmc.2020.115976.

References

1 Siegel RL, Miller KD, Jemal A. Cancer statistics, 2020. *CA Cancer J Clin.* 2020;70:7–30. https://doi.org/10.3322/caac.21590.
2 Nazmy EA, El-Khouly OA, Zaki MMA, et al. Targeting p53/TRAIL/caspase-8 signaling by adiponectin reverses thioacetamide-induced hepatocellular carcinoma in rats. *Environ Toxicol Pharmacol.* 2019;72, 103240. https://doi.org/10.1016/j.etap.2019.103240.
3 Modi SJ, Kulkarni VM. Vascular Endothelial Growth Factor Receptor (VEGFR-2)/KDR Inhibitors: Medicinal Chemistry Perspective. *Med Drug Discov.* 2019;2, 100009. https://doi.org/10.1016/j.medidd.2019.100009.
4 Kamal A, Lakshma Nayak V, Nagesh N, Vishnuvardhan MVPS, Subba Reddy NV. Benzo[b]furan derivatives induces apoptosis by targeting the PI3K/Akt/mTOR signaling pathway in human breast cancer cells. *Bioorg Chem.* 2016;66:124–131. https://doi.org/10.1016/j.bioorg.2016.04.004.
5 Lu JM, Zhang ZZ, Ma X, Fang SF, Qin XH. Repression of microRNA-21 inhibits retinal vascular endothelial cell growth and angiogenesis via PTEN dependent-PI3K/Akt/VEGF signaling pathway in diabetic retinopathy. *Exp Eye Res.* 2020;190, 107886. https://doi.org/10.1016/j.exer.2019.107886.
6 Amour A, Barton N, Cooper AWJ, et al. Evolution of a Novel, Orally Bioavailable Series of PI3KΔ Inhibitors from an Inhaled Lead for the Treatment of Respiratory Disease. *J Med Chem.* 2016;59:7239–7251. https://doi.org/10.1021/acs.jmedchem.6b00799.
7 FDA approves first PI3K inhibitor for breast cancer | FDA, (n.d.). https://www.fda.gov/news-events/press-announcements/fda-approves-first-pi3k-inhibitor-breast-cancer (accessed April 12, 2020).
8 Bursavich MG, Brooijmans N, Feldberg L, et al. Novel benzofuran-3-one indole inhibitors of PI3 kinase-α and the mammalian target of rapamycin: Hit to lead studies. *Bioorgan Med Chem Lett.* 2010;20:2586–2590. https://doi.org/10.1016/j.bmcl.2010.02.082.
9 Sieuwerts AM, Inda MA, Smid M, et al. ER and PI3K Pathway Activity in Primary ER Positive Breast Cancer Is Associated with Progression-Free Survival of Metastatic Patients under First-Line Tamoxifen. *Cancers (Basel).* 2020;12:802. https://doi.org/10.3390/cancers12040802.
10 Vasan N, Toska E, Scaltriti M. Overview of the relevance of PI3K pathway in HR-positive breast cancer. *Ann Oncol Off J Eur Soc Med Oncol.* 2019;30:x3–x11. https://doi.org/10.1093/annonc/mdz281.
11 Ioannilli L, Ciccarone F, Ciriolo MR. Adipose Tissue and FoxO1: Bridging Physiology and Mechanisms. *Cells.* 2020;9:849. https://doi.org/10.3390/cells9040849.
12 Antimicrobial resistance, (n.d.). https://www.who.int/en/news-room/fact-sheets/detail/antimicrobial-resistance (accessed March 23, 2019).

13 Cassini A, Högberg LD, Plachouras D, et al. a population-level modelling analysis. *Lancet Infect Dis.* 2015;19(2019):56–66. https://doi.org/10.1016/S1473-3099(18)30605-4.

14 Kirilmis C, Ahmedzade M, Servi S, Koca M, Kizirgil A, Kazaz C. Synthesis and antimicrobial activity of some novel derivatives of benzofuran: Part 2. The synthesis and antimicrobial activity of some novel 1-(1-benzofuran-2-yl)-2-mesitylethanone derivatives. *Eur J Med Chem.* 2008;43:300–308. https://doi.org/10.1016/j.ejmech.2007.03.023.

15 Mehdi SH, Hashim R, Ghalib RM, et al. Synthesis, characterization, antimicrobial and enzymatic activity of 4b,9b-dihydroxy-7,8-dihydro-4bH-indeno[1,2-b]benzofuran-9,10(6H,9bH)-dione. *J Mol Struct.* 2011;1006:318–323. https://doi.org/10.1016/j.molstruc.2011.09.026.

16 Kokare DG, Kamat V, Naik K, Nevrekar A, Kotian A, Revankar VK. Evaluation of DNA cleavage, antimicrobial and anti-tubercular activities of potentially active transition metal complexes derived from 2,6-di(benzofuran-2-carbohydrazono)-4-methylphenol. *J Mol Struct.* 2017;1127:289–295. https://doi.org/10.1016/j.molstruc.2016.07.072.

17 Rangaswamy J, Vijay Kumar H, Harini ST, Naik N. Synthesis of benzofuran based 1,3,5-substituted pyrazole derivatives: As a new class of potent antioxidants and antimicrobials-A novel accost to amend biocompatibility. *Bioorgan Med Chem Lett.* 2012;22:4773–4777. https://doi.org/10.1016/j.bmcl.2012.05.061.

18 Miller MB, Bassler BL. Quorum Sensing in Bacteria. *Annu Rev Microbiol.* 2001;55:165–199. https://doi.org/10.1146/annurev.micro.55.1.165.

19 Bhardwaj AK, Vinothkumar K, Rajpara N. Bacterial Quorum Sensing Inhibitors: Attractive Alternatives for Control of Infectious Pathogens Showing Multiple Drug Resistance. *Recent Pat Antiinfect Drug Discov.* 2013;8:68–83. https://doi.org/10.2174/1574891x11308010012.

20 El-Gohary NS, Shaaban MI. New pyrazolopyridine analogs: Synthesis, antimicrobial, antiquorum-sensing and antitumor screening. *Eur J Med Chem.* 2018;152:126–136. https://doi.org/10.1016/j.ejmech.2018.04.025.

21 Bérubé G. An overview of molecular hybrids in drug discovery. *Exp Opin Drug Discov.* 2016;11:281–305. https://doi.org/10.1517/17460441.2016.1135125.

22 Papoutsi Z, Kassi E, Papaevangeliou D, et al. Plant 2-arylobenzofurans demonstrate a selective estrogen receptor modulator profile. *Steroids.* 2004;69:727–734. https://doi.org/10.1016/j.steroids.2004.07.005.

23 dos Santos Silva TD, Bomfim LM, da Cruz Rodrigues ACB, et al. Anti-liver cancer activity in vitro and in vivo induced by 2-pyridyl 2,3-thiazole derivatives. *Toxicol Appl Pharmacol.* 2017;329:212–223. https://doi.org/10.1016/j.taap.2017.06.003.

24 Xue DQ, Zhang XY, Wang CJ, et al. Synthesis and anticancer activities of novel 1,2,4-triazolo[3,4-a] phthalazine derivatives. *Eur J Med Chem.* 2014;85:235–244. https://doi.org/10.1016/j.ejmech.2014.07.031.

25 Abulkhair HS, Turky A, Ghiaty A, Ahmed HEA, Bayoumi AH. Novel triazolophthalazine-hydrazone hybrids as potential PCAF inhibitors: Design, synthesis, in vitro anticancer evaluation, apoptosis, and molecular docking studies. *Bioorg Chem.* 2020;100, 103899. https://doi.org/10.1016/j.bioorg.2020.103899.

26 Kyei SK, Akaranta O, Darko G. Synthesis, characterization and antimicrobial activity of peanut skin extract-azo-compounds. *Sci African.*. 2020, e00406 https://doi.org/10.1016/j.sciaf.2020.e00406.

27 Manojkumar P, Ravi TK, Gopalakrishnan S. Antioxidant and antibacterial studies of arylazopyrazoles and arylhydrazonopyrazolones containing coumarin moiety. *Eur J Med Chem.* 2009;44:4690–4694. https://doi.org/10.1016/j.ejmech.2009.07.004.

28 Samad MK, Hawaiz FE. Synthesis, characterization, antioxidant power and acute toxicity of some new azo-benzamide and azo-imidazolone derivatives with in vivo and in vitro antimicrobial evaluation. *Bioorg Chem.* 2019;85:431–444. https://doi.org/10.1016/j.bioorg.2019.01.014.

29 Okasha RM, Alsehli M, Ihmaid S, et al. First example of Azo-Sulfa conjugated chromene moieties: Synthesis, characterization, antimicrobial assessment, docking simulation as potent class I histone deacetylase inhibitors and antitumor agents. *Bioorg Chem.* 2019;92, 103262. https://doi.org/10.1016/j.bioorg.2019.103262.

30 Coşkun D, Tekin S, Sandal S, Coşkun MF. Synthesis, Characterization, and Anticancer Activity of New Benzofuran Substituted Chalcones. *J Chem.* 2016;2016:1–8. https://doi.org/10.1155/2016/7678486.

31 Liu J, Yi W, Wan Y, Ma L, Song H. 1-(1-Arylethylidene)thiosemicarbazide derivatives: A new class of tyrosinase inhibitors. *Bioorgan Med Chem.* 2008;16:1096–1102. https://doi.org/10.1016/j.bmc.2007.10.102.

32 Gautam D, Gautam P, Chaudhary RP. N-Methylpyridinium tosylate catalyzed green and efficient synthesis of some novel 2,4-disubstituted thiazoles and 4-thiazolidinones. *Chin Chem Lett.* 2012;23:1221–1224. https://doi.org/10.1016/j.cclet.2012.10.002.

33 Shehzad MT, Khan A, Islam M, et al. Synthesis, characterization and molecular docking of some novel hydrazonothiazolines as urease inhibitors. *Bioorg Chem.* 2020;94, 103404. https://doi.org/10.1016/j.bioorg.2019.103404.

34 Salman AS, Mahmoud NA, Mohamed MA, Abdel-Aziem A, Elsisi DM. Synthesis, Characterization and in vitro Cytotoxic Evaluation of Some Novel Heterocyclic Compounds Bearing Indole Ring. *Asian J Org Med Chem.* 2017;2:42–52. https://doi.org/10.14233/ajomc.2017.ajomc-p66.

35 Dabholkar VV, Parmar BM. *Synthesis and Antibacterial Activity of Some Novel Substituted.* 2011;1:35–42. https://doi.org/10.1016/j.annfar.2012.02.019.

36 Riyadh SM. Enaminones as building blocks for the synthesis of substituted pyrazoles with antitumor and antimicrobial activities. *Molecules.* 2011;16:1834–1853. https://doi.org/10.3390/molecules16021834.

37 Al-Zaydi KM, Borik RM, Elnagdi MH. 2-Arylhydrazonopropanals as building blocks in heterocyclic chemistry: Microwave assisted condensation of 2-aryl-hydrazono-propanals with amines and active methylene reagents. *Molecules.* 2003;8:910–923. https://doi.org/10.3390/81200910.

38 Gaber HM, Bagley MC, Muhammad A, Gomha SM. RSC Advances Recent developments in chemical reactivity of N , N - dimethylenamino ketones as synthons for various heterocycles, (2017) 14562–14610. https://doi.org/10.1039/c7ra00683g.

39 Radfar I, Abbasi S, Miraki MK, Yazdani E, Karimi M, Heydari A. Glycerol-K2CO3 Deep Eutectic Solvent as Environmentally Friendly Media with Basic and Dehumidifier Synergistic Effect for Running of Willgerodt-Kindler Reaction. *ChemistrySelect.* 2018;3:3265–3267. https://doi.org/10.1002/slct.201702906.

40 Daidone G, Raffa D, Plescia F, Maggio B. Synthesis of pyrazole-4-carbohydrazide derivatives of pharmaceutical interest, 2002 (2002) 227–235.

41 Kamble A, Kamble R, Dodamani S, et al. Design, synthesis and pharmacological analysis of 5-[4′-(substituted-methyl)[1,1′-biphenyl]-2-yl]-1H-tetrazoles. *Arch Pharm Res.* 2017;40:444–457. https://doi.org/10.1007/s12272-017-0887-0.

42 Skey J, O'Reilly RK. Facile one pot synthesis of a range of reversible addition-fragmentation chain transfer (RAFT) agents. *Chem Commun.* 2008:4183–4185. https://doi.org/10.1039/b804260h.

43 Lal K, Kaushik CP, Kumar K, et al. One-pot synthesis and cytotoxic evaluation of amide-linked 1,4-disubstituted 1,2,3-bistriazoles. *Med Chem Res.* 2014;23:4761–4770. https://doi.org/10.1007/s00044-014-1038-5.

44 Cao S-L, Han Y, Yuan C-Z, et al. Synthesis and antiproliferative activity of 4-substituted-piperazine-1-carbodithioate derivatives of 2,4-diaminoquinazoline. *Eur J Med Chem.* 2013;64:401–409. https://doi.org/10.1016/J.EJMECH.2013.04.017.

45 Cacic M, Trkovnik M, Cacic F, Has-Schon E. Synthesis and Antimicrobial Activity of Some Derivatives of (7- Hydroxy-2-oxo-2. *Molecules.* 2006;11:134–147. https://doi.org/10.7598/cst2013.478.

46 Maira SM, Stauffer F, Schnell C, García-Echeverría C. PI3K inhibitors for cancer treatment: Where do we stand? *Biochem Soc Trans.* 2009;37:265–272. https://doi.org/10.1042/BST0370265.

47 El-Gohary NS, Shaaban MI. Design, synthesis, antimicrobial, antiquorum-sensing and antitumor evaluation of new series of pyrazolopyridine derivatives. *Eur J Med Chem.* 2018;157:729–742. https://doi.org/10.1016/j.ejmech.2018.08.008.

48 Furet P, Guagnano V, Fairhurst RA, et al. Discovery of NVP-BYL719 a potent and selective phosphatidylinositol-3 kinase alpha inhibitor selected for clinical evaluation. *Bioorgan Med Chem Lett.* 2013;23:3741–3748. https://doi.org/10.1016/j.bmcl.2013.05.007.

49 Daina A, Michielin O, Zoete V. SwissADME: A free web tool to evaluate pharmacokinetics, drug-likeness and medicinal chemistry friendliness of small molecules. *Sci Rep.* 2017;7:1–13. https://doi.org/10.1038/srep42717.

50 Russo M. Filippo; Ghelardoni, New thiazole compounds containing the benzofuran system. *Ann Chim.* 1964;54:987–1000.

51 Abdelhamid AO, Ismail ZH, Abdel-Aziem A. Reactions with Hydrazonoyl Halides 60 1: Synthesis of Thieno[2′,3′:4,5] Pyrimidino[1,2- b][1,2,4,5]tetrazines, [1] benzothieno[2′,3′:4,5]pyrimidino [1,2- b][1,2,4,5]tetrazines, Pyrazolo[3′,4′:4,5] pyrimidino[1,2- b] [1,2,4,5]tetrazines and Pyrazolo[3,4- d]pyridazines. *J Chem Res.* 2007;2007:609–616. https://doi.org/10.3184/030823407X256118.

52 Abdelhamid AO, Fahmi AA, Alsheflo AAM. Convenient synthesis of some new pyrazolo[5,1-c]triazines, isoxazolo[3,4-d] pyrimidine and pyridine derivatives containing benzofuran moiety. *Eur J Chem.* 2012;3:129–137. https://doi.org/10.5155/eurjchem.3.2.129-137.579.

53 McClean KH, Winson MK, Fish L, et al. Quorum sensing and Chromobacterium violaceum: Exploitation of violacein production and inhibition for the detection of N-acylhomoserine lactones. *Microbiology.* 1997;143:3703–3711. https://doi.org/10.1099/00221287-143-12-3703.

54 McLean RJC, Pierson LS, Fuqua C. A simple screening protocol for the identification of quorum signal antagonists. *J Microbiol Methods.* 2004;58:351–360. https://doi.org/10.1016/j.mimet.2004.04.016.